Supporting Information

Table of Contents

I. General procedures and materials for experimental methods.

All reactions were performed with dry solvents except where noted. All glasswares were either oven- or flame-dried and the reactions were performed under a slight positive pressure of inert gas such as N_2 or Ar unless otherwise noted. All chemicals were commercially purchased. Compounds were purified by normal phase flash chromatography on silica gel unless otherwise noted. NMR spectra were collected on a Varian MR400 premium shielded magnet, with either a Varian 5 mm AutoX dual broadband probe or Varian autoswitchable quad probe. ^{1}H and ^{13}C drifts were corrected against residual solvent peaks[1]; ^{19}F were corrected using trifluoroacetic acid (δ = -76.5 ppm) as a standard in some cases. NMR spectra were analyzed using Mestrenova software. Low-resolution mass spectra were obtained on a Micromass LCT time-of-flight (TOF) instrument with electrospray ionization (ESI) coupled to a HPLC pump with a rheodyne loop injector. High-resolution mass spectra were collected on an Agilent Q-TOF (accuracy 1–5 ppm) with in-line photodetector array, either in direct-injection mode or through a Waters 10 cm C18 column with a 5–95% water:acetonitrile gradient, 5 mL/min for 15 min. All gel-based biochemical experiments were performed as technical replicates (from the same AhpC bacterial lysate stock) 2 or more times, each time in duplicate. TIRF imaging experiments were performed as 3 separate biological replicates performed on separate days. Confocal imaging experiments were performed as 3 technical replicates. Sample size was dictated largely by initial pilot experiments, followed by secondary experiments for higher quality analysis typically yielding 2 or more independent replicates.

Fluorescence Spectroscopy. All spectroscopy was done in Hellma Analytics quartz precision cells 10 x 2 mm. Fluorescence spectra were collected on a Varian Cary Eclipse fluorescence

spectrophotometer with 5 nm excitation and emission slit widths. Absorbance measurements were collected on a Varian Cary 100 Bio UV-visible spectrophotometer. Lucifer yellow (Sigma-Aldrich) was used as a quantum yield standard by matching absorbance to DiNap at the excitation maxima, and integrating the emission intensity, correcting for refractive index as necessary.

HPLC analysis. High-performance liquid chromatography separations were performed on a Waters HPLC 1525 binary pump system with an in-line Waters 2707 autosampler, reverse-phase column, Waters 2998 photodiode array (PDA), and Waters fraction collector III. Samples were injected and run through an Atlantis prep T3 (10 x 250 mm) C_{18} column equilibrated at 5% acetonitrile/water (0.10% formic acid), held at this solvent composition for 1 min, and linearly increased to 95% until 12 min, and held at this solvent composition for 1 min before being re-equilibrated to 5% acetonitrile : water. Solvent elution was 5 mL/min. Absorption spectra were collected through the PDA, and data were analyzed using Waters Empower software. Elution traces were collected at the approximate maximum wavelength for each compound (dimedone: 280 nm; DiNaps 488 nm).

SDS-PAGE analysis. Samples were either combined immediately with loading buffer and heated to 95˚C for 10–15 min, or, as necessary, small molecules were removed by a modified trichloroacetic acid (TCA) precipitation. Briefly, proteins were precipitated by adding 0.2 volumes of a 50% w/v mixture of TCA/water, centrifuged (1000 x g for 3 minutes), and the supernatant was removed. Next, the protein pellet was sonicated and washed in cold methanol (3x) and acetone (1x), and resuspended in 6 M urea in SDS gel loading buffer. Proteins were separated using pre-cast 12% acrylamide gels (BioRad) run at 160 V for 70 minutes. Western blots were transferred to Millipore Immobulon FL paper with 100 V input over 70 minutes. We found that for all probes tested, there significant retention in the polyacrylamide gel. To prevent this, samples were either first processed by TCA precipitation or transferred to PVDF membranes for direct fluorescence analysis. The following antibodies were used in this study: mouse α-His_6 (Qiagen, 34660), mouse α-GAPDH (EMD Millipore, CB1001), mouse α-E-cadherin (BD Bioscience, 610181), rabbit anti-β-actin (Cell Signaling Technologies, 4967S). All DiNap gel-based imaging was performed using a GE Typhoon Scanner equipped with a 488 nm laser line and 555/20 nm emission filter. Near-infrared western blot imaging was performed with an Azure Biosystems c600 system.

Mammalian cell culture. HeLa, HEK293T, and MDA-MB-231 cells were grown in DMEM media with 10% FBS and penicillin/streptomycin. There was no additional authentication of HeLa or HEK293T cells, which are listed in the database of commonly misidentified cell lines maintained by ICLAC (http://iclac.org/databases/cross-contaminations/) and used only for retroviral packaging or

comparative F-DiNap labeling. A431 cells were cultured similarly and were a gift from Morand Piert (Michigan). CH27 cells were grown in DMEM media with 15% FBS with L-Glutamine, 1 g/L glucose, and 110 mg/L sodium pyruvate with penicillin/streptomycin in the presence of 50 μM 2-mercaptoethanol. MCF10A (provided by Benjamin Margolis, Michigan) cells were transduced with retrovirus produced from pPGS-hSnail-fl.Flag-NEO (Addgene plasmid no. 25695) and pCL-Ampho packaging vector. After two days, cells were selected with 600 μg/ml G418 (Life Technologies). MCF10A vector and Snail1 cells were cultured in DMEM/F12 base medium (Thermo) supplemented with 5% dialyzed horse serum, 20 ng/ml recombinant human epidermal growth factor (Shenandoah), 0.5 mg/ml hydrocortisone (Sigma), 100 ng/ml cholera toxin (Sigma), and 10 μg/ml insulin (Sigma). After probe incubation, cells were washed 3x with Dulbecco's Phosphate Buffered Saline (DPBS) and mechanically scraped from the dish. Protein levels were quantified prior to SDS-PAGE using the DC protein assay (BioRad).

Cloning and Mutagenesis of E.coli AhpC and human GAPDH. Whole genomic DNA was extracted from Top10 E.coli using TRIzol Reagent (Life Technologies) according to manufacturer's protocol. TRIzol reagent was also used to extract RNA from HEK293T cells. cDNA was synthesized from 1 μg of total RNA using SuperScriptIII reverse transcriptase (Life Technologies). The bacterial gene for AhpC (Uniprot ID: P0AE08) was amplified from *E. coli* genomic DNA using Phusion DNA polymerase chain reaction (PCR), with primers containing BamHI and XhoI restriction sites (underlined) (5'-TTTGGATCCGTCCTTGATTAACACCAAAATTAA-3', 5'-TTTCTCGAGTTAGATTTTACCAACCAGGTCC-3'). Human GAPDH was amplified from HEK293t cDNA with the primers 5'-TTTGGATCCGGGGAAGGTGAAGGTCGGAGTC -3' and 5'-TTTCTCGAGTTACTCCTTGGAGGCCATGTG-3' containing BamHI and XhoI restriction enzyme sites (underlined). After restriction enzyme digestion, each the AhpC and GAPDH fragment was ligated (T4 DNA ligase, NEB) into pET45b between BamHI and XhoI sites to insert an N-terminal His tag. The AhpC-C166S mutant was created by quick change site-directed mutagenesis with primers 5'-CACCCAGGTGAAGTTTCCCCGGCTAAATGGAAAG-3' and 5'-CTTTCCATTTAGCCGGGGAAACTTCACCTGGGTG-3' and confirmed by DNA sequencing.

Expression and Purification of AhpC-C166S and GAPDH. For large-scale recombinant expression in bacteria, 1 L of TB media with 50 μg/mL carbenicillin was inoculated with the appropriate BL21 strain and grown with shaking at 250 rpm at 37 °C. When the OD_{600} = 0.6, the cultures were induced with 0.5 mM IPTG and temperature was reduced to 22 °C. After shaking for 16 hours, *E. coli* were harvested by centrifugation. Pellets were stored at -80 °C until purification. All purification steps were carried out at 4 °C. To frozen (-80 °C) pellets from 1 L of *E. coli* culture

grown in TB, 40 mL of lysis buffer (50 mM Tris pH 8.0, 150 mM NaCl, 10% glycerol) was added. Pellets were lysed by sonication, and cell debris was pelleted by centrifugation at 12,000 x g for 30 minutes. The lysate was frozen for future use, or AhpC or GAPDH was purified from the supernatant using TALON (Clontech) resin according to manufacturer's protocol. Fractions containing the desired recombinant protein (as indicated by SDS-PAGE) were pooled and transferred to dialysis tubing (10,000 MWC), and dialyzed into 20 mM Tris pH 8.0 with 30 mM NaCl to remove imidazole. Protein was concentrated using 10,000 MWC spin concentrators, aliquoted and stored at -80 °C.

Labeling rate calculations. Rate reactions were performed in parallel using PCR strip tubes and a multichannel pipette. A 2.5 mg /mL solution of cleared E.coli lysate overexpressing AhpC-His_6 C166S was prepared in tris-buffered saline (TBS) buffer, pH 7.4. These samples were reacted with a 20X stock of either H- or F-DiNap at a final concentration of 0.2, 0.4, 0.8, 1.6, 3.2, and 6.4 mM in 150 µL. At the indicated time points, 8 µL of the reaction mixture was transferred into the PCR tube containing 8 µL of 8 M urea (freshly prepared) and 4 µL of a 5x Laemali SDS-PAGE sample buffer containing β-mercaptoethanol. These strips were immediately transferred to a PCR thermocycler that had been preheated to 90 ˚C with a 100 ˚C lid to prevent condensation, and left to denature for 5 minutes. Denatured samples were then placed on ice until all the time points were complete. 10 µL of each sample was then loaded onto a 15-well SDS PAGE 12% polyacrylamine gel, transferred to a PDVF membrane. The membranes were blocked with BSA (5% solution in TBS-T with 0.01% NaN_3), followed by addition of the primary mouse anti-His_6 antibody (in 5% BSA in TBS-T with 0.01% NaN_3) and secondary donkey anti-mouse with Alexa Fluor® 647 (in TBS-T with 0.01% NaN_3). The DiNap was imaged with 488 ex/555 em and loading controls with 633 ex/670 em. The fluorescence of the Ahpc-His_6 C166S protein bands were quantified using ImageJ, and protein loading was normalized using either coomassie blue staining or anti-His_6 immunostaining and the pseudo first-order rates were fit to a second order k_{rxn} using a global fit in GraphPad Prism 7.0.

TIRF microscopy. Cells were plated on 35 mm #1.5 glass-bottomed culture dishes (MatTek Corporation, Ashland, MA). Cells were incubated with 1 mM H-DiNap or F-DiNap in Tyrode's buffer to avoid labeling of any other proteins in serum, like albumin. Imaging was performed on an Olympus IX81-XDC inverted microscope with a cellTIRF module, a 100X UAPO TIRF objective (NA=1.49), and active Z-drift correction (ZDC) (Olympus America, Center Valley, PA). Images were acquired on an iXon-897 EMCCD camera (Andor, South Windsor, CT). TIRF excitation was accomplished using a 488 nm diode laser (Sapphire 488 LP, Coherent) and a 402 nm diode laser (CUBE 405-50FP, Coherent). Excitation intensities were adjusted to give approximately equal

emission between UV and blue excitation. Data was processed to subtract the non-specific background, and ratios were calculated by diving the 488 nm intensity by the 405 nm intensity. Excitation and emission was filtered using the quadband dichroic mirror LF405/488/561/635-4X-A-000 (Semrock, Lake Forest, IL). Images were analyzed using MATLAB (The MathWorks, Natick, MA).

Confocal microscopy. Cells were plated on #1.5 glass-bottomed culture dishes and imaged on a Nikon A1R+ laser scanning confocal microscope with a 60 × 1.4 Plan Apo VC oil objective. Cells were incubated with 1 mM F-DiNap in growth media for 15 minutes and imaged without washing. Sequential excitation was accomplished using 405- and 488-nm lasers, and emission was gathered through a 500-550 nm bandpass filter using a pinhole diameter of 116.2 microns. A stage-top humidified incubation chamber (Okolab) was used to maintain the cells at 37 °C and 5% CO_2. Z-stacks were captured using an optical thickness of 375 nm in Z. Exposures were adjusted to the maximum dynamic range while avoiding saturation. Images were analyzed with NIS-Elements AR software (Nikon).

Peroxide Survival Assay (Resorufin-AM). MCF10A and MCF10A-Snail cell lines were seeded at 5000 cells/well in 96-well culture plates and incubated at 37°C. The following day, cells were treated with 0, 50, 100, 150, 200, 250, 300, 350, 400 nM final concentration of H_2O_2 in 1x DPBS (20 µL) added directly to the medium. Cells incubated for 30 min at 37 °C before aspirating medium, washed with 1x DPBS (100µL) and replaced with fresh growth medium (80 µL). Following this treatment, cells were left to recover at 37 °C for 23 hours. The medium was then aspirated, washed with 1x DPBS (100 µL), and 80 µL of 1x DPBS was added to each well. Next, a 10 µM solution of resorufin-AM in 1x DPBS (20 µL) to each well for 1 h at 37 °C. Resorufin-AM was synthesized according to published methods[2]. The fluorescent emission of activated resorufin-AM was measured at 590/10 nm with excitation at 535/25 nm. The average background fluorescence from a cell-free control was then subtracted from all wells and the average fluorescence for each condition normalized to the untreated control. All conditions were performed as 6 replicates.

II. Synthetic Schemes

Scheme S1. Mechanistic rationale for α-substituted active methylene compounds.

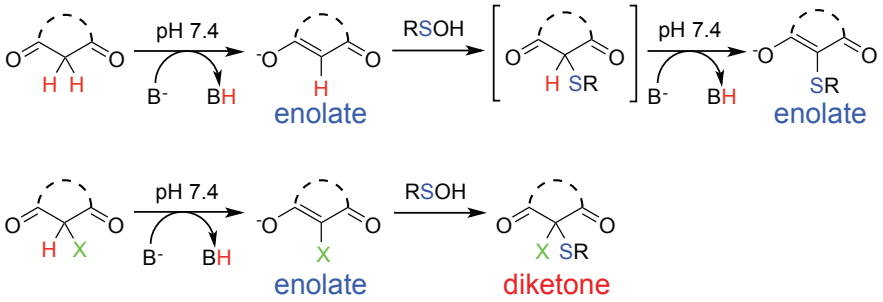

In cyclic 1,3-diketones such as dimedone, the pK_a of the α-proton is below physiological pH and predominantly exists in enol form in aqueous solution, which can react with a sulfenic acid to form a thioether. The second α-proton is acidic enough to undergo second deprotonation after sulfenic acid conjugation. From this mechanism, it is clear that the first α-deprotonation step is necessary for the reaction, but the second plays no role in sulfenic acid conjugation. Therefore, replacement of one of the α-protons with a small blocking group (Me, F) would trap the sulfenic acid-conjugated product in the diketone form. This enolate-to-diketone transition might switch the chemical and electronic properties of a conjugated dye to provide a direct approach for live-cell imaging of this dynamic redox post-translational modification.

Scheme S2. Conversion of 4-bromo-1,8-naphthalic anhydride to DiNapBr (**2a**–**c**).

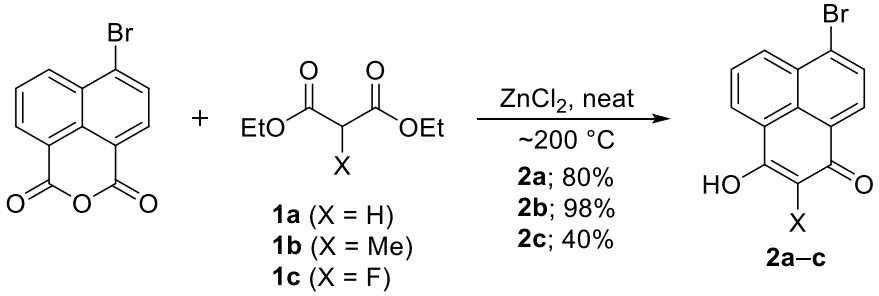

1a (X = H)
1b (X = Me)
1c (X = F)

2a–**c**

Using a modified literature procedure[3], a suspension of anhydrous zinc chloride (3.0 equiv) in thionyl chloride (20 mL) was refluxed for 30 min. The thionyl chloride was removed by rotary evaporation until the zinc chloride appeared as a free-flowing white powder. Then 4-bromo-1,8-naphthalic anhydride (1.0 equiv) and diethyl malonate **1** (10 equiv) were added to the flask equipped with a reflux condenser and the mixture was heated at ~200 °C for 6 h. unreacted diethyl malonate was removed by vacuum distillation and the solid cake obtained was crushed, washed with 1 N HCl, and filtered. The resulting solid was dissolved in a 1:1 mixture of MeOH and 1 N NaOH and filtered to remove unwanted solid particles. The clear filtrate was precipitated with 6 N HCl and the crude DiNapBr precipitate was filtered and then driedunder vacuum. The dried solid

was washed with DCM few times to remove residual malonate and naphthalic anhydride. The crude product obtained as solid powder was carried forward to the next amination reaction.
Note: DiNap compounds have poor solubility in commonly used organic solvents, and are thus difficult to purify by standard chromatographic techniques. A highly pure sample could not be obtained in all cases.

7-Bromo-3-hydroxy-1H-phenalen-1-one (H-DiNapBr, 2a). Zinc chloride (3.0 equiv, 7.38 g, 54 mmol), 4-bromo-1,8-naphthalic anhydride (1.0 equiv, 5.00 g, 18 mmol), and diethyl malonate (10 equiv, 27.5 mL, 181 mmol) were used as described. 3.95 g (80%) of crude **2a** was obtained. ^{1}H NMR (400 MHz, DMSO-d_6) δ 8.34 (dd, *J* = 8.4, 1.2 Hz, 1H), 8.30 (dd, *J* = 7.3, 1.2 Hz, 1H), 8.04 (m, 2H), 7.83 (dd, *J* = 8.5, 7.3 Hz, 1H), 6.13 (s, 1H). ^{13}C NMR (100 MHz, DMSO-d_6) δ 174.4, 173.8, 131.5, 130.8, 130.1, 128.3, 128.2, 128.1, 127.8, 127.8, 127.1, 126.3, 105.3. ESI-MS for $C_{13}H_8BrO_2$: [M+H] 274.9702 (predicted 274.9708).

7-Bromo-3-hydroxy-2-methyl-1H-phenalen-1-one (Me-DiNapBr, 2b). Zinc chloride (3.0 equiv, 6.87 g, 50 mmol), 4-bromo-1,8-naphthalic anhydride (1.0 equiv, 4.66 g, 17 mmol), and diethyl 2-methylmalonate (10 equiv, 28.6 mL, 168 mmol) were used as described. 4.76 g (98%) of crude **2b** was obtained. ^{1}H NMR (400 MHz, DMSO-d_6) δ 8.05 (d, *J* = 6.7 Hz, 1H), 7.95 (d , *J* = 8.1 Hz, 1H), 7.79 (d, *J* = 7.5Hz, 1H), 7.70 (d, *J* = 7.6 Hz, 1H), 7.52 (t, *J* = 7.1 Hz, 1H), 1.94 (s, 3H). ^{13}C NMR (100 MHz, DMSO-d_6) δ 163.2, 163.1, 130.4, 130.3, 129.4, 127.8, 127.5, 127.2, 127.1, 126.6, 126.2, 125.8, 113.1, 8.8. ESI-MS for $C_{14}H_{10}BrO_2$: [M+H] 288.9857 (predicted 288.9864). NMR purity >75%.

7-Bromo-2-fluoro-3-hydroxy-1H-phenalen-1-one (F-DiNapBr, 2c). Zinc chloride (3.0 equiv, 22.1 g, 160 mmol), 4-bromo-1,8-naphthalic anhydride (1.0 equiv, 15.0 g, 54 mmol), and diethyl fluoromalonate (5.0 equiv, 48 g, 270 mmol) were used as described. 6.50 g (40%) of crude **2c** was obtained. ^{1}H NMR (400 MHz, CD_3OD) δ 8.52 (dd, *J* = 8.5, 0.80 Hz, 1H),, 8.46 (dd, *J* = 7.3, 0.80 Hz, 1H),, 8.22 (d, *J* = 7.9 Hz, 1H), 8.04 (d, *J* = 7.9 Hz, 1H), 7.82 (t, *J* = 7.9 Hz, 1H). ^{13}C NMR (100 MHz, DMSO-d_6) δ 142.8, 140.4, 133.5, 133.1, 131.8, 131.0, 129.7, 128.9, 128.6, 128.2, 126.7, 125.9, 124.4. ^{19}F NMR (377 MHz, CD_3OD) δ –164.8. ESI-MS for $C_{13}H_7BrFO_2$: [M+H] 292.9611 (292.9613 predicted).

Scheme S3. General procedure for conversion of DiNapBr (**2a**–**c**) to DiNap (**3a**–**c**).

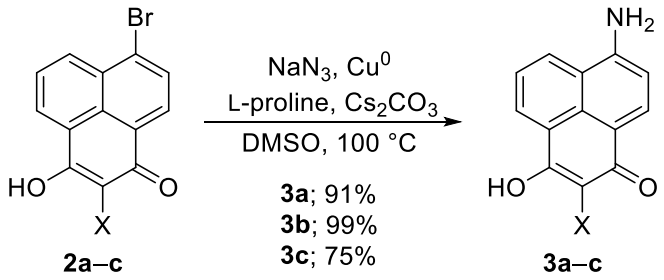

Using a modified literature procedure[4], anhydrous DMSO (30 mL) was purged with nitrogen under vacuum using sonication for 15 min to remove dissolved gases. To a flame-dried Schlenk flask under nitrogen atmosphere was added **2** (1.0 eq) followed by copper metal (1.1 eq), sodium azide (3.0 eq), L-proline (1.4 eq), and cesium carbonate (2.5 equiv). The flask was then purged under a steady stream of nitrogen for at least 15 min. Degassed DMSO was then added to the Schlenk flask containing all the reagents and the mixture was heated at 100 °C for 6 h. The reaction was cooled to room temperature and 6 N HCl was added until a fluffy red precipitate was produced. The solid was filtered, washed with 1 N HCl, and the solid was eluted with methanol. Purification of the crude product via flash silica gel chromatography using 0–10% MeOH/DCM gradient afforded sufficiently pure products.

7-Amino-3-hydroxy-1*H*-phenalen-1-one (H-DiNap, 3a). Starting with **2a** (1.95 g), 1.37 g (91%) of the title compound was isolated. The ^{1}H and ^{13}C NMRs spectra matched with the spectra of **3a** synthesized using an alternate route (see below)

7-Amino-3-hydroxy-2-methyl-1*H*-phenalen-1-one (Me-DiNap, 3b). Starting with **2b** (1.0 g), 0.769 g (99%) of the title compound was isolated. ^{1}H NMR (400 MHz, DMSO-d_6) δ 9.39 (brs, 2H), 8.86 (d, *J* = 8.0 Hz, 1H), 8.67 (d, *J* = 7.6Hz, 1H), 8.53 (d, *J* = 9.0 Hz, 1H), 7.70 (t, *J* = 7.9 Hz, 1H), 6.93 (d, *J* = 9.0 Hz, 1H), 2.17 (s, 3H). ^{13}C NMR (101 MHz, DMSO-d_6) δ 170.5, 163.7, 158.6, 137.2, 137.1, 131.4, 130.5, 125.7, 124.3, 122.5, 119.8, 111.79, 111.75, 9.5. ESI-MS for $C_{14}H_{12}NO_2$: $[M+H]^+$ 226.0863 (predicted 226.0868).NMR purity >90%.

7-Amino-2-fluoro-3-hydroxy-1*H*-phenalen-1-one (F-DiNap, 3c). Starting with **2c** (0.506 g), 0.395 g of **3c** was obtained, which was >85% pure by NMR. Spectroscopic data of a pure sample is reported below (see alternate synthesis of **3c**).

*Initial biological studies were performed with **3c** synthesized using the methods described above. However, the synthesis was not reproducible in later efforts. Thus, an alternate synthetic route was implemented to procure enough **3c** for further studies and feasibility of this route was also demonstrated for the synthesis of **3a**.*

Scheme S4. Alternate synthesis of F-DiNap (**3c**)

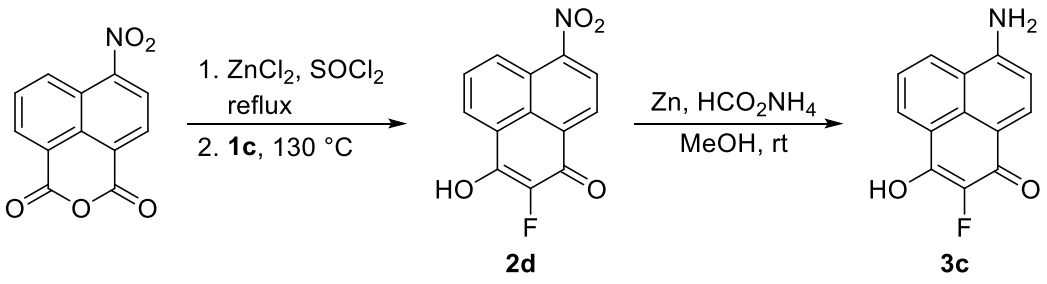

2d **3c**

2-Fluoro-3-hydroxy-7-nitro-1*H*-phenalen-1-one (F-DiNap-NO_2, 2d). A suspension of 4-nitro-1,8-naphthalic anhydride (1.00 g, 4.11 mmol, 1.0 equiv) and zinc chloride (1.68 g, 12.3 mmol, 3.0 equiv,) in 50 mL thionyl chloride was refluxed for two hours. The thionyl chloride was removed via rotary evaporation and to the flask was added diethyl fluoromalonate **1c** (7.30 g, 41.0 mmol, 10 equiv) at once and the reaction mixture was heated at 130 ˚C for 4 hours. The reaction mixture was cooled to room temperature and ground with DCM in a mortar. The suspension was filtered and the grinding in DCM was repeated with the remaining solid several times until the filtrate was colorless. The solid so obtained was dissolved in 1 N NaOH solution and the fine suspension was filtered to remove greyish-purple precipitate. The filtrate was acidified with concentrated HCl yielding a brick-red precipitate, which was filtered and then washed with water. The precipitate was dried and then suspended in dichloromethane. The suspension was added to the top of an addition funnel that was layered with glass wool, Celite, and sand. Refluxing DCM was then allowed to pass through the solid facilitating the extraction. Once clear filtrate was observed, the extraction was stopped and the DCM layer was washed three times with sat. $NaHCO_3$ solution. The combined red-colored aqueous layer was washed once with DCM followed by acidification with 1 N HCl to yield an orange precipitate. The precipitate was filtered and washed with 1 N HCl. The solid on the filter paper was dissolved in methanol. Rotary evaporation of the solvent afforded 118 mg of the crude product, which was used as such for the next reduction reaction. NMR showed residual MeOH peak. ^{1}H NMR (400 MHz, DMSO-d_6) δ 8.58 (d, J = 8.7 Hz, 1H), 8.47–8.39 (m, 3H), 7.99 (t, J = 8.0 Hz, 1H); ^{13}C NMR (126 MHz, DMSO-d_6) δ 148.8, 142.0 (d, *J* = 242.5 Hz, 1C), 130.3 (d, *J* = 4.4 Hz, 1C), 129.8 (2C), 129.6, 128.6, 126.9, 126.7 (d, *J* = 5.3 Hz, 1C), 124.3, 124.1 (2C), 122.8; ^{19}F NMR (377 MHz, DMSO-d_6) δ –158.6; ESI-MS for $C_{13}H_5FNO_4$: $[M–H]^–$ 258.0203 (predicted 258.0208).

7-Amino-2-fluoro-3-hydroxy-1H-phenalen-1-one (F-DiNap, 3c). To a solution of **2d** (14.0 mg, 0.0540 mmol, 1.0 equiv) in MeOH (2.0 mL) was added ammonium formate (17.0 mg, 0.270 mmol, 5.0 equiv). To the resulting red solution was added zinc powder (35.3 mg, 0.540 mmol, 10 equiv) and the reaction mixture was allowed to stir atroom temperature for 2 h under N_2. The reaction was filtered to remove zinc, and the residue was rinsed thoroughly with methanol. The filtrate was

collected and the solvent was removed by rotary evaporation. The resulting solid was boiled in DCM and the suspension was filtered. The DCM layer was discarded and the resulting solid was finely supended in hot acetone and filtered through a plug of Celite and silica. More acetone was added to flush the product out until the brown-colored baseline started to move on the silica. The solvent was concentrated and the residue was dissolved in sat. $NaHCO_3$ solution. The aqueous layer was washed once with DCM followed by acidification with 1 N HCl. The suspension was sonicated and filtered. The reddish-orange solid was washed with 1 N HCl and was eluted off with methanol. Concentration of MeOH followed by vacuum drying afforded 5.6 mg of the product that was sufficiently pure by NMR. ^{1}H NMR (400 MHz, CD_3OD) δ 8.52–8.47 (m, 2H). 8.31 (d, *J* = 8.7 Hz, 1H), 7.63 (t, *J* = 7.9 Hz, 1H), 6.85 (d, *J* = 8.7 Hz, 1H); ^{13}C NMR (126 MHz, DMSO-d_6) δ 154.0, 141.9 (d, *J* = 237.5 Hz, 1C), 132.7 (d, *J* = 2.6 Hz, 1C), 127.7 (d, *J* = 6.4 Hz), 127.2, 125.0, 124.3, 123.5 (2C), 119.4, 114.4, 108.8 (2C); ^{19}F NMR (377 MHz, CD_3OD) δ –165.1; ESI-MS for $C_{13}H_9FNO_2$: $[M+H]^+$ 230.0613 (predicted 230.0617).

Scheme S5. Alternate synthesis of H-DiNap (**3a**)

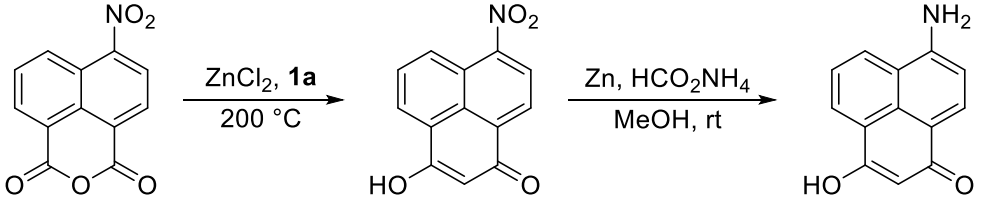

2e **3a**

3-Hydroxy-7-nitro-1*H*-phenalen-1-one (H-DiNap-NO_2, 2e). To an oven dried 25 mL RBF flushed with Ar and equipped with a condenser was taken anhydrous zinc chloride (350 mg, 2.57 mmol, 5.0 equiv) followed by the addition of 4-nitro-1,8-naphthalic anhydride, 95% (125 mg, 0.514 mmol, 1.0 equiv) and diethyl malonate (0.780 mL, 5.14 mmol, 10 equiv). The reaction mixture was heated at 200 °C for 5 h under Ar. The reaction mixture was cooled toroom temperature and the brown solid obtained was suspended in 1 N HCl, sonicated, and filtered. The solid thus obtained was dissolved in a 1:1 mixture of MeOH and 1 N NaOH and the resulting reddish-brown fine suspension was filtered through Celite followed by washings with 1 N NaOH/MeOH mixture. The combined filtrate was acidified with 6 N HCl to yield dark red precipitate. The suspension was filtered and the dark red solid was washed with water several times and dried under vacuum. The dried solid was then suspended in DCM and filtered. The solid was washed with DCM and again dried under vacuum to yield 124 mg of crude **2e**, which was used as such for the next reduction reaction. ^{1}H NMR (400 MHz, DMSO-d_6) δ 8.56 (d, *J* = 8.6 Hz, 1H), 8.36–8.46 (m, 3H), 7.98 (dd, *J* = 8.7, 7.3 Hz, 1H), 6.09 (s, 1H); ^{13}C NMR (126 MHz, DMSO-d_6) δ 149.1, 130.9, 130.0 (2C), 129.0, 128.1, 127.8, 127.4, 126.4, 124.3 (2C), 123.4, 106.3; ESI-MS for $C_{13}H_8NO_4$: $[M+H]^+$ 242.0449 (predicted 242.0453)

7-Amino-3-hydroxy-1*H*-phenalen-1-one (H-DiNap, 3a). To a brownish-orange suspension of **2e** (17.0 mg, 0.0705 mmol, 1.0 equiv) in MeOH (1.0 mL) in a N_2-flushed 1 dram vial was added activated zinc powder (18.4 mg, 0.282 mmol, 4.0 equiv) followed by ammonium formate (11.1 mg, 0.176 mmol, 2.5 equiv) and the resulting reaction mixture was stirred at room temperature for 1 h. The reaction mixture was filtered through a plug of Celite bed and the bright orange filtrate (with a green fluorescence) was concentrated under N_2. The residue was triturated and sonicated with DCM (1.0 mL) twice and the DCM layer was decanted. The brownish-orange sticky residue was dried under vacuum and then suspended in deionized water (0.70 mL). After sonication, the orange suspension was centrifuged at 5000 rpm for 1.5 min and the supernatant was decanted. This process was repeated once more. The resulting wet solid was dried under vacuum. Purification of this crude solid on a Combiflash using a 12 g normal-phase silica flash column and a solvent gradient of 0–10% MeOH/DCM afforded an impure product. Further purification of this impure product on a Combiflash using a 30 g HP C18 gold column with a solvent gradient of 0–100% ACN in water afforded slightly impure product as an orange-red solid after drying under vacuum. This slightly impure product was dissolved in acetonitrile with few drops of MeOH and filtered through a cotton plug. The filtrate was concentrated to yield a sufficiently pure product (6.0 mg, 40%) as a bright orange crystalline solid after drying under vacuum. ^{1}H NMR (500 MHz, DMSO-d_6) δ 8.46 (d, J = 8.2 Hz, 1H), 8.21 (d, J = 7.2 Hz, 1H), 8.01 (d, J = 8.2 Hz, 1H), 7.53 (t, J = 7.8 Hz, 1H), 7.11 (s, 2H), 6.73 (d, J = 8.3 Hz, 1H), 5.81 (s, 1H); ^{13}C NMR (126 MHz, DMSO-d_6) δ 152.0, 131.0 (2C), 128.6, 127.0 (3C), 123.3 (2C), 120.1, 107.7 (2C), 104.3; ESI-MS for $C_{13}H_{10}NO_2$: $[M+H]^+$ 212.0707 (predicted 212.0712).

Scheme S6. General procedure to synthesize conjugated DiNap dye standards.

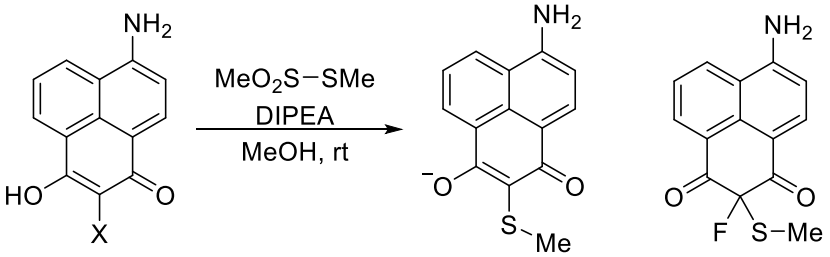

3a (X = H)
3c (X = F)

4a (36%)

4c (37%)

To a solution or suspension of DiNap **3** (1.0 equiv) in methanol (5 mL) atroom temperature was added *N*,*N*-diisopropylethylamine (DIPEA) (1.2 equiv) followed by *S*-methyl methanethiosulfonate (MMTS) (1.1 equiv), and the reaction was allowed to stir overnight atroom temperature. The

reaction mixture was adsorbed on the silica gel and then purified by flash chromatography using a gradient of 0–5% MeOH/DCM.

MeS-DiNap (4a). Starting with 86 mg of **3a**, 38 mg (36%) of **4a** was isolated. ^{1}H NMR (400 MHz, DMSO-d_6) δ 10.06 (s, 1H), 8.53 (d, *J* = 8.2 Hz, 1H), 8.33 (d, *J* = 7.0 Hz, 1H), 8.12 (d, *J* = 8.4 Hz, 1H), 7.60 (t, *J* = 7.8 Hz, 1H), 7.36 (s, 2H), 6.78 (d, *J* = 8.4 Hz,1H), 2.22 (s, 3H). ^{13}C NMR (100 MHz, DMSO-d_{66}) δ 152.9 (2C), 132.6 (2C), 128.6, 127.9 (2C), 127.7, 123.6 (2C), 119.9, 108.1 (2C), 17.1; ESI-MS for $C_{14}H_{12}NO_2S$: $[M+H]^+$ 258.0583 (predicted 258.0589).

MeS-F-DiNap (4c). Starting with 40 mg of **3c**, 18 mg (37%) of **4c** was isolated. ^{1}H NMR (400 MHz, CD_3OD) δ 8.45 (dd, *J* = 8.4, 1.2 Hz, 1H), 8.32 (dd, *J* = 7.2, 1.2 Hz, 1H), 8.20 (d, *J* = 8.4 Hz, 1H), 7.65–7.56 (m, 1H), 6.88 (d, *J* = 8.4 Hz, 1H), 2.19 (d, *J* = 2.3 Hz, 3H). ^{19}F NMR (377 MHz, CD_3OD) δ –167.06; ESI-MS for $C_{14}H_{11}FNO_2S$: $[M+H]^+$ 276.0486 (predicted 276.0495); for $C_{14}H_{10}FNO_2SNa$: $[M+Na]^+$ 298.0307 (predicted 298.0314).

III. Supplementary Tables

Table S1. Fluorescence properties of DiNap probes.

Compound	No.	Excitation λ_{max} (nm)	Emission λ_{max} (nm)	solvent	ε (M^{-1} cm^{-1})	Φ (QY)
H-DiNap	3a	453	542	PBS	10270	0.175
Me-DiNap	3b	470	542	PBS	6490	0.070
F-DiNap	3c	472	544	PBS	8720	0.069
H-MeS-DiNap	4a	458	542	PBS	8680	0.031
F-MeS-DiNap	4c	448	543	MeOH	7030	0.029

IV. Supplementary Figures

Figure S1. F-DiNap and Dyn-2 label a similar profile of proteins.

BL21 lysates (100 µg in 100 µL) overexpressing Ahpc C166S were incubated with 5 mM of F-DiNap or DYn2 for 1 hr. The reaction was stopped by TCA precipitation, at which point the DYn-2 sample was treated with 1 mM $CuSO_4$, 1 mM TCEP, 1 mM Tris[(1-benzyl-1H-1,2,3-triazol-4-yl)methyl]amine, and 50 µM TAMRA-azide, and analyzed by SDS-PAGE. Although there were minor differences, the overall profile was very similar.

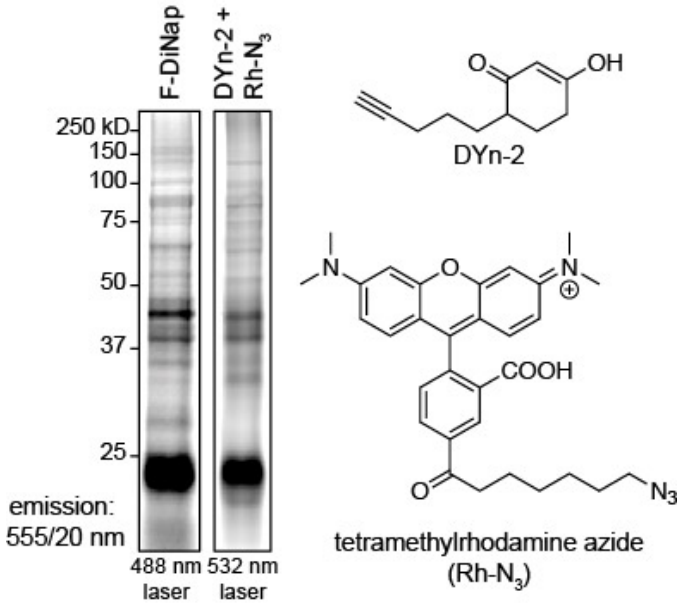

Figure S2. Reaction of **3c** in an oxidation-dependent manner.

F-DiNap labeling of AhpC (C166S) is oxidation dependent, nearly eliminating labeling after treatment with 5 mM TCEP for 1 hour. A very marginal increase is observed after peroxide treatment, indicating that most of the protein is present in the oxidized state in the bacterial cell lysates. NT = no treatment.

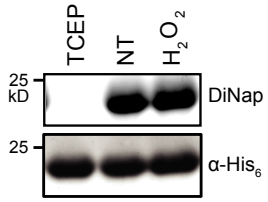

Figure S3. F-DiNap reacts with a cyclic sulfenamide.

A cyclic sulfenamide MeOVal-CysSA-Cbz was prepared using a literature procedure[5]. DiNap **3c** (100 mM stock in DMSO; final concentration of 1 mM) was added to the sulfenamide (100 mM stock in DMSO; final concentration of 1 mM) was reacted in DPBS for 1 hr. HPLC analysis reveals the formation of a new species.

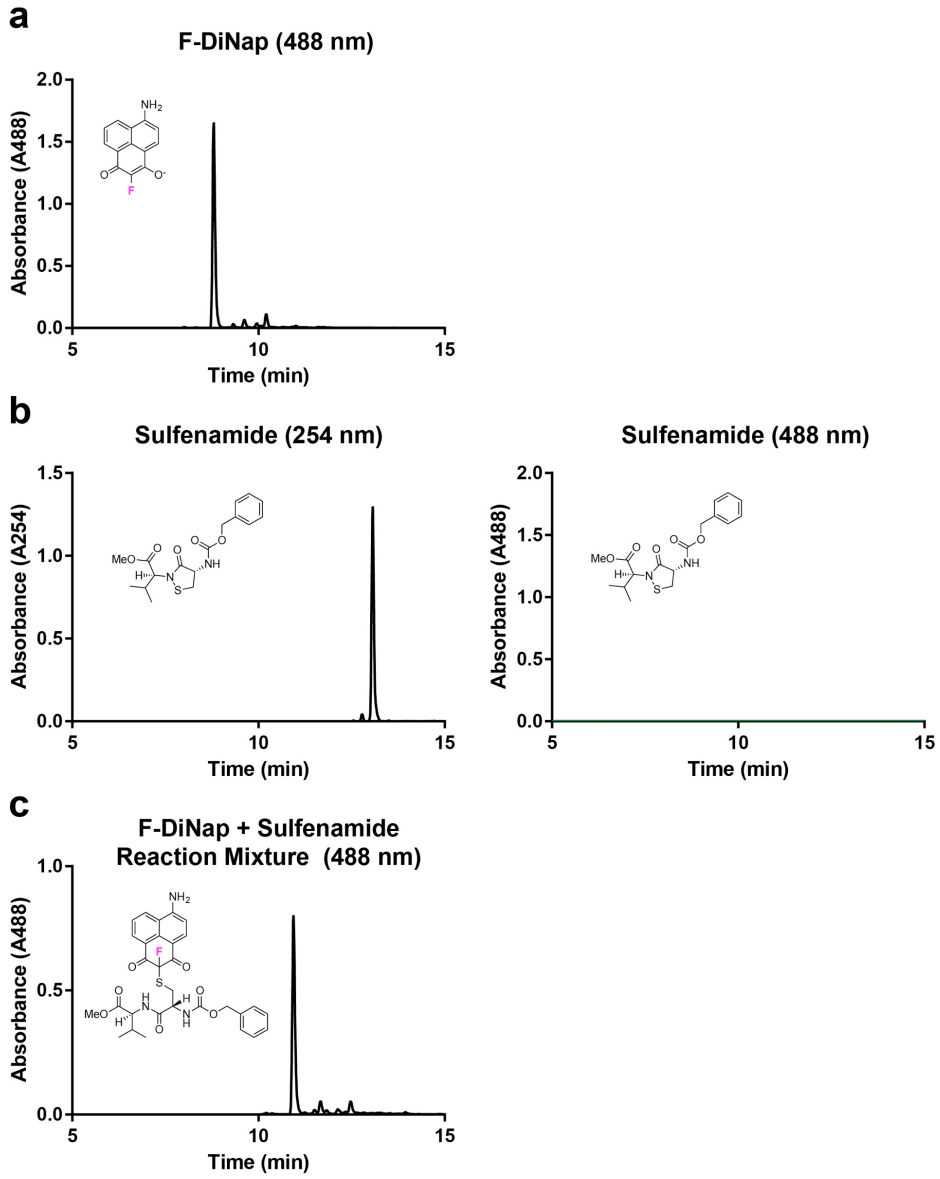

Figure S4. F-DiNap shows a significant ^{19}F NMR shift upon conjugation in aqueous buffer. To a mixture of 10% D_2O in DPBS (pH 7.4) was added with 33 μM trifluoroacetic acid (TFA) and DiNap **3c** (100 mM stock in DMSO; final concentration, 1 mM). (**a**) The ^{9}F NMR of F-DiNap and TFA. (**b**) Subsequently the cyclic sulfenamide MeOVal-CysSA-Cbz (100 mM stock in DMSO; final concentration, 1 mM) was reacted for 1 hr with F-DiNap. (**c**) Fluorine is sensitive to chemical environment, and F-DiNap shifts from -170.52 to -120.69 ppm upon reaction.

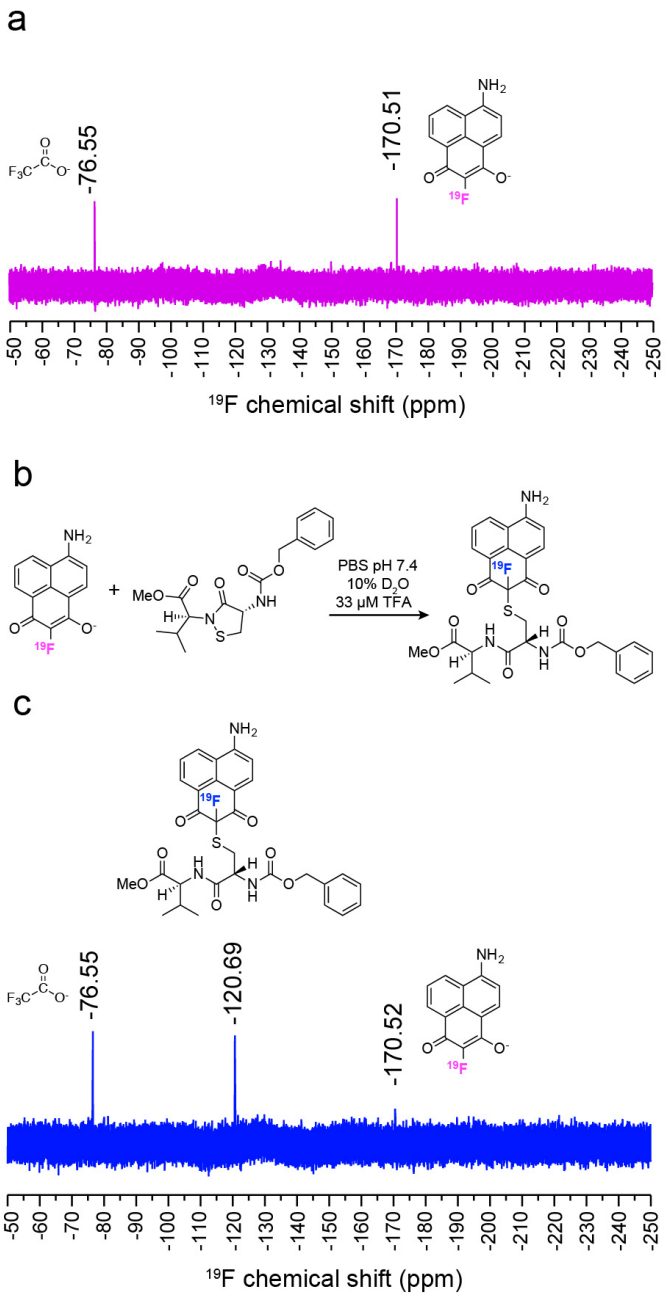

Figure S5. F-DiNap changes its fluorescence excitation spectra below the probe pKa. Data is normalized to 1 to highlight changes in the peak excitation. Excitation spectra were collected by monitoring emission intensity at 550 nm.

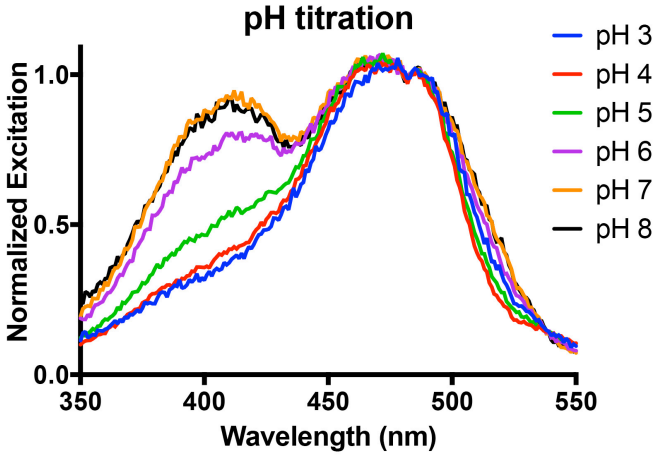

Figure S6. DiNap probe pK_a values.
Measurements were acquired from 100 µM solutions of each DiNap probe in buffered solutions at the defined pH values. The ratio of the 488 nm fluorescence excitation intensity was divided by the 405 nm excitation intensity, plotted and fit to sigmoidal curve with the half-max inflection point taken as the pK_a.

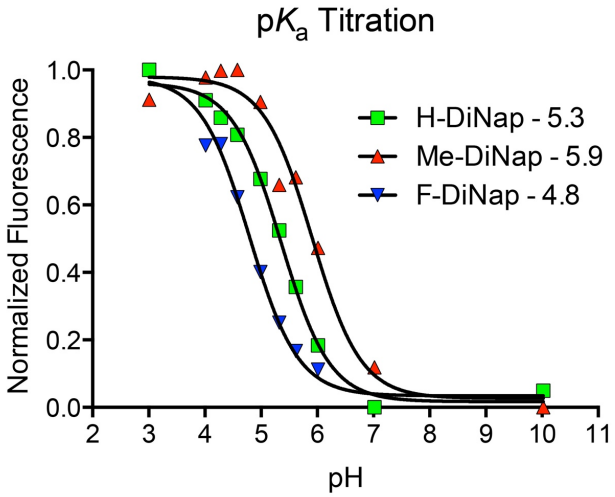

Figure S7. Fluorescence spectra of **3a** and **4a**.

The 400 nm excitation of **3a** is reduced after conjugation to the sulfenic acid analogue methylmethane thiosulfonate (MMTS) (**4a**). We hypothesize the free enolate electrons donate into the empty *d*-orbitals of sulfur, which can alter absorption from the 1,3-dione portion of the molecule.

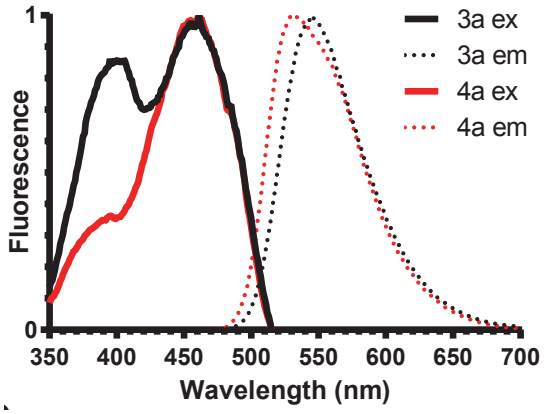

Figure S8. Ratiometric response to sulfenic acid addition.

F-DiNap demonstrates an excitation ratiometric response to MeOVal-CysSA-Cbz in PBS:Acetonitrle (2:1) that saturates at 2 equivalents. Measurements were acquired after 10 minutes.

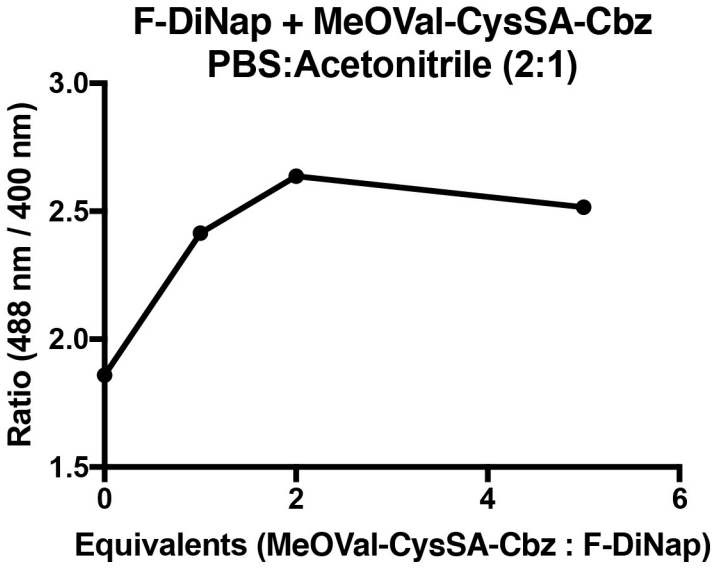

Figure S9. Rate calculations for H- and F-DiNap on AhpC (C166S).

Calculated rate values by in-gel fluorescence of AhpC (C166S) in bacterial lysates. k_{rxn} of H-DiNap with Ahpc C166S: 0.683 ± 0.085 M^{-1} s^{-1}; k_{rxn} of F-DiNap with Ahpc C166S 1.71 ± 0.45 M^{-1} s^{-1}.

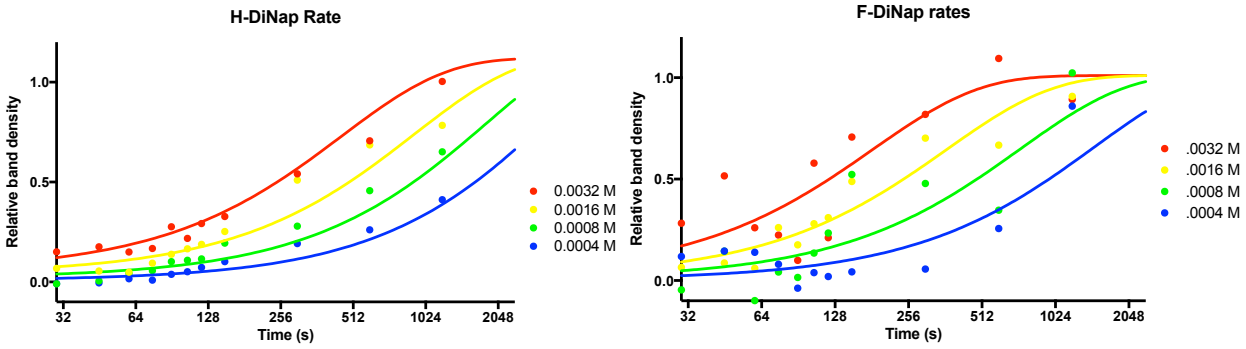

Figure S10. Representative images for the gels. Raw data was used for rate calculations. H- and F-DiNap were tested with E.coli lysates overexpressing Ahpc-His_6 C166S. Variation in image quality is due to using different imaging systems.

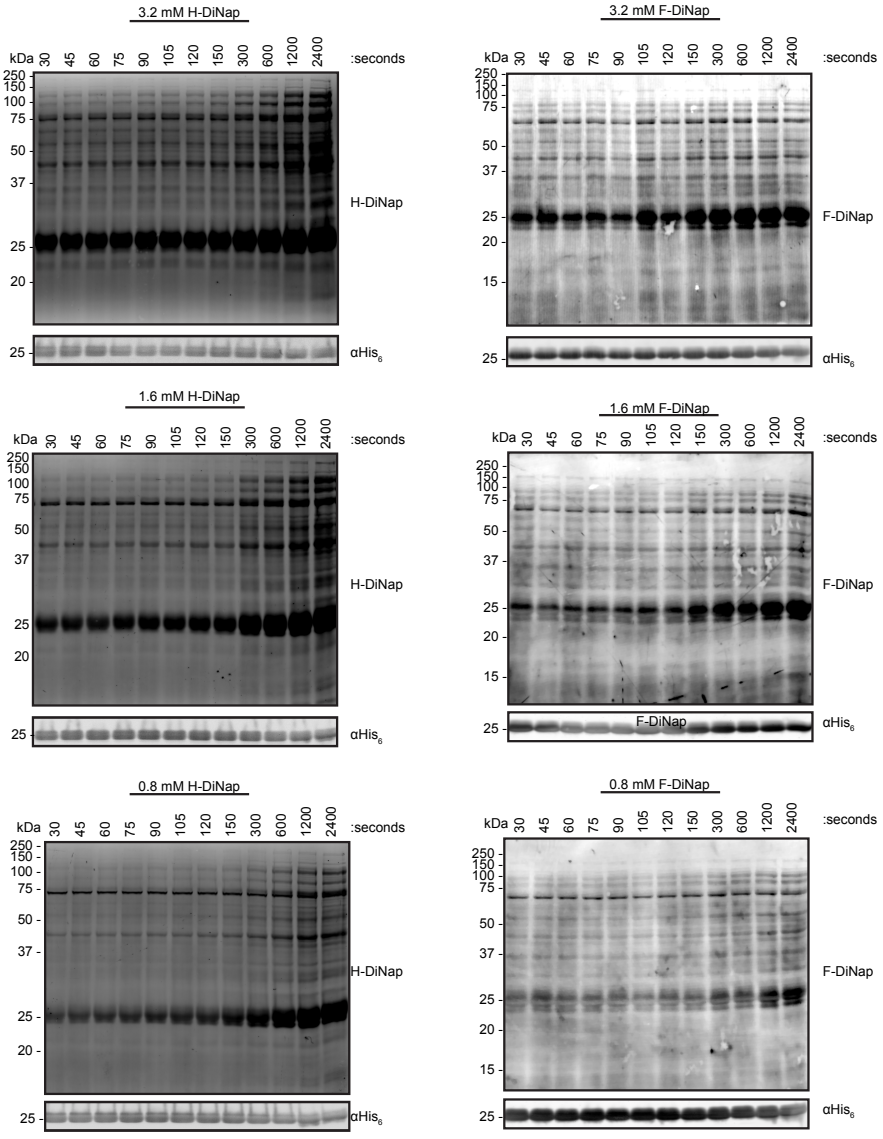

Figure S11. Dimedone reacts with pyridoxal.

Dimedone (5 mM final) or F-DiNap (5 mM final) and pyridoxal (15 mM final) were added in DPBS, incubated for 30 minutes, and subsequently analyzed by HPLC using a photodiode array detector. The same solution was analyzed on LC-HRMS to confirm the presence of the single and double adduct.

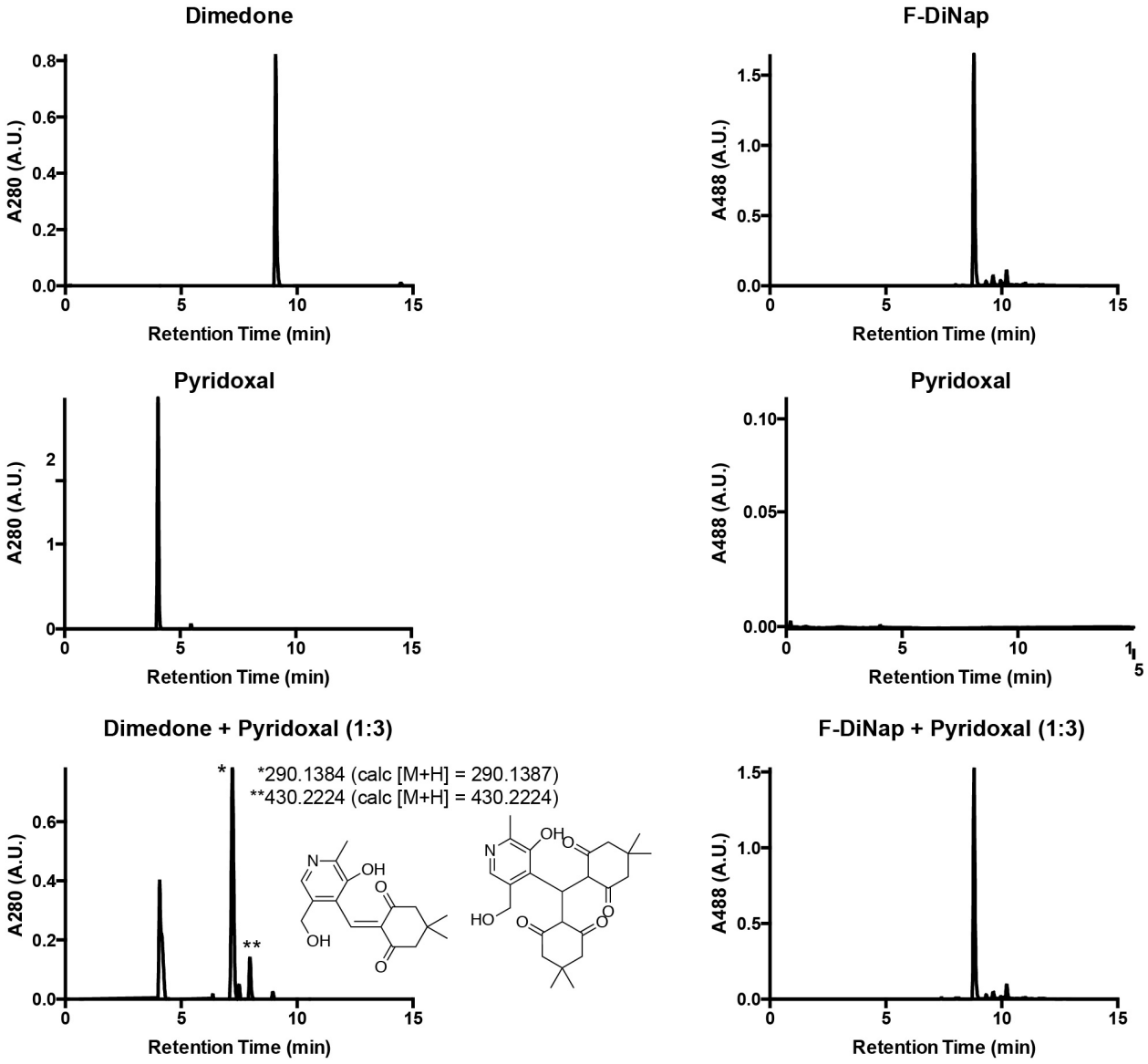

Figure S12. Dimedone reacts with glyceraldehyde.

Dimedone (5 mM final) or F-DiNap (5 mM final) and glyceraldehyde (15 mM final) were added in DPBS, incubated for 30 minutes, and subsequently by HPLC using a photodiode array detector. The same solution was analyzed on LC-HRMS to confirm the presence of the single adduct.

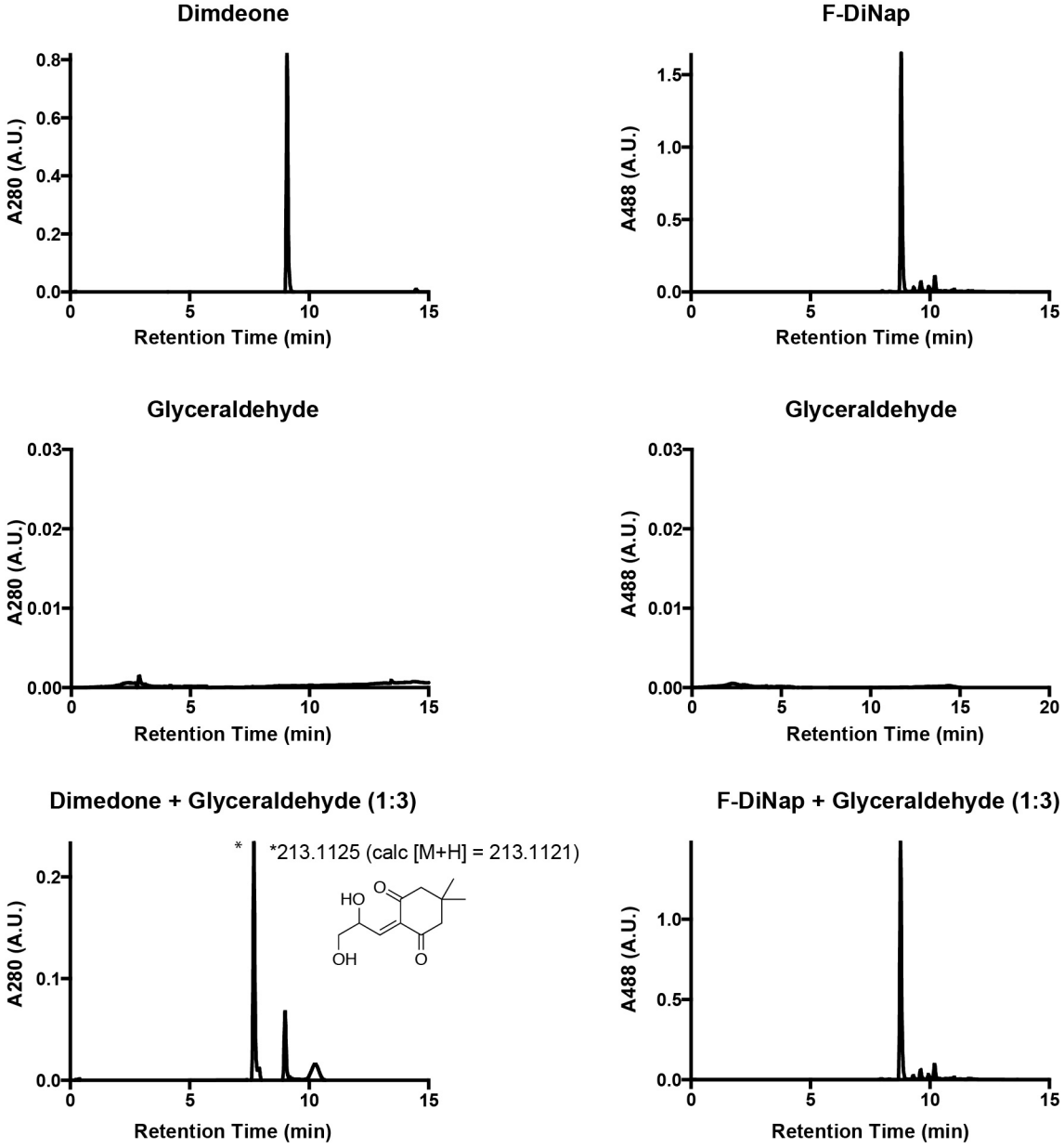

Figure S13. Reaction rate of glyceraldehyde and dimedone in phosphate buffer.
Dimedone (0.5 mM final concentration) was added to DPBS in an HPLC vial. To this was added a solution of from stock solutions of glyceraldehyde at 5, 10, 15, 20, 30, 40, 80 and 160 mM final concentrations. Aliquots were removed by HPLC and initial t = 0 was run, and then subsequent time points at 15 minute intervals using the standard methods. The area under the dimedone curve at 280 nm was measured and collected. These data were globally fit, yielding a rate constant of 0.104 ± 0.006 M^{-1} s^{-1}.

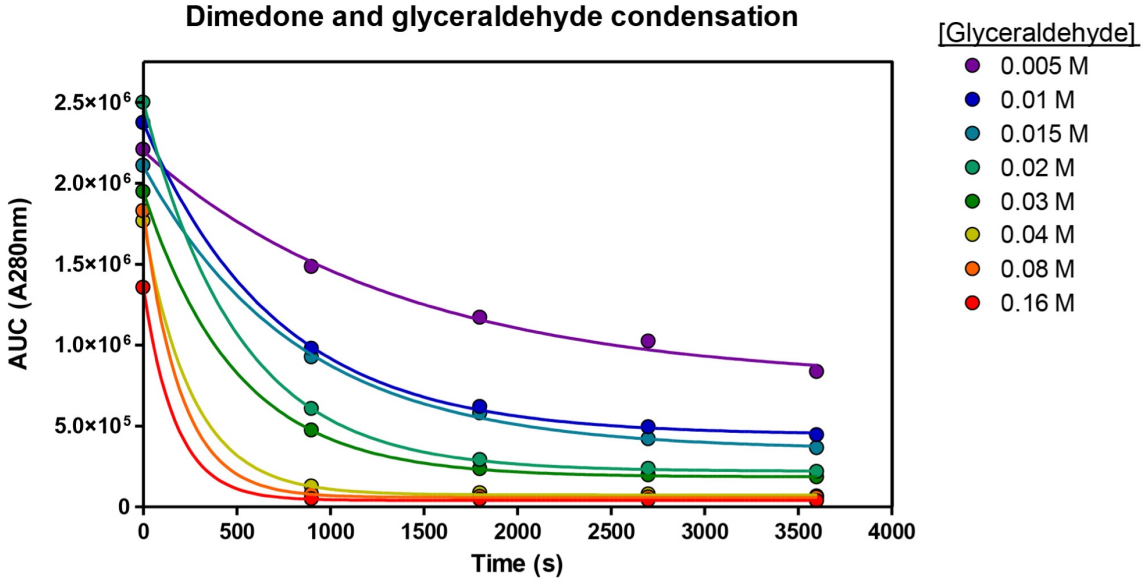

Substrate Consumption Via One-Step Pseudo First Order Bimolecular		
	Best-fit values	Std. Dev
krxn (1/M/s)	0.1041	0.00632

Figure S14. Dimedone reacts with ene-als.

Dimedone (5 mM final) or F-DiNap (5 mM final) and acrolein or acrolein + N-acetyl cysteine (5 mM final each) were added in DPBS, incubated for 30 minutes, and analyzed using by HPLC using a photodiode array detector.

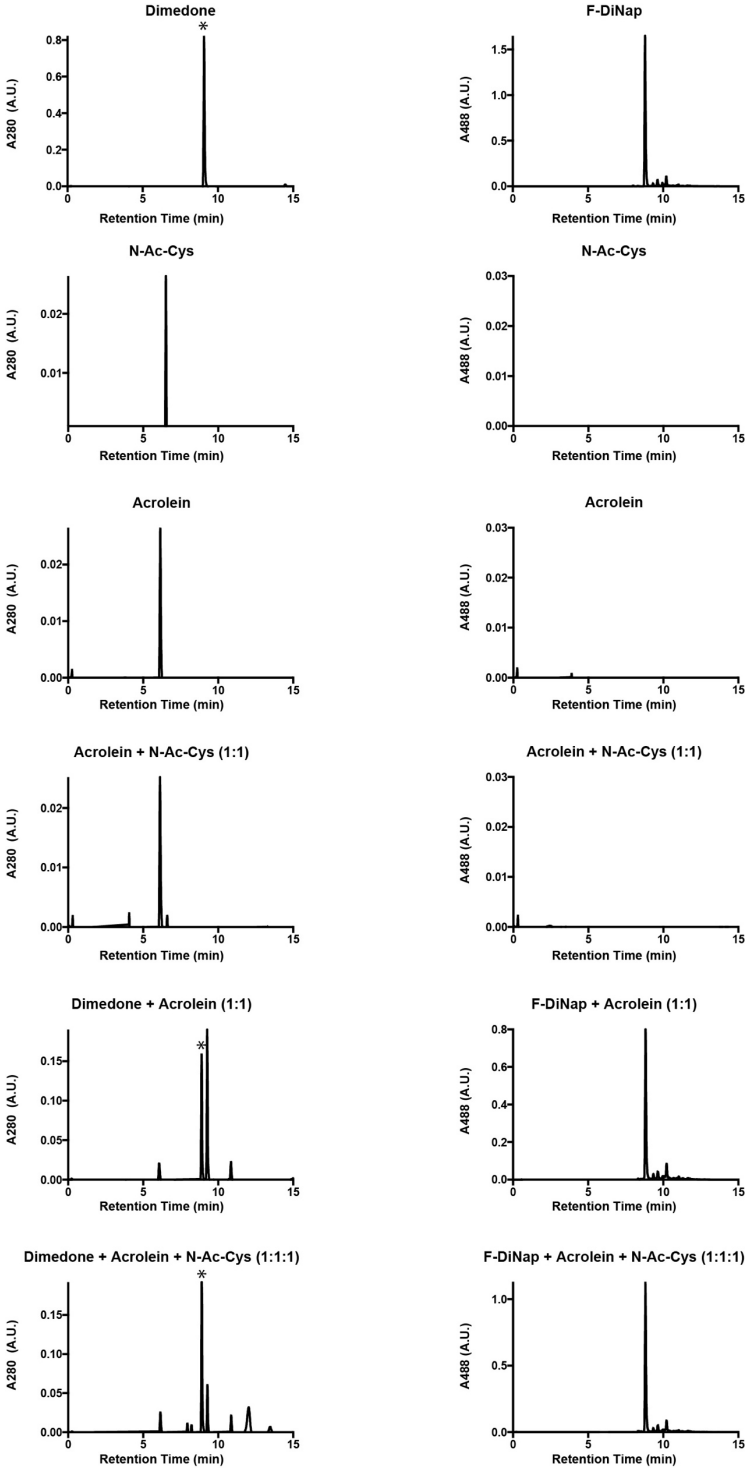

Figure S15. F-DiNap does not react with ene-als.

Bacterial lysates were incubated with 1 mM of either acrolein or 4-hydroxynonenal for 30 minutes, followed by addition of 5 mM H- or F-DiNap for 60 minutes.

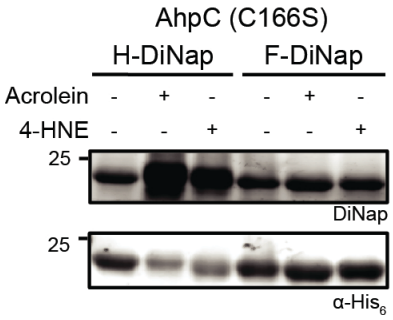

Figure S16. F-DiNap profiling of *S*-sulfenylation in different cell lines.

Cells were labeled with F-DiNap (5 mM) for 1 hour at 37 ˚C, washed with DPBS, collected by scraping form the dish, and lyzed by sonication. After normalizing for protein concentration, lysates were separated by SDS-PAGE and transferred to PVDF membrane for GAPDH western blotting (Cy5) and F-DiNap (Ex: 488 nm, Em: 555/20 nm) fluorescence imaging.

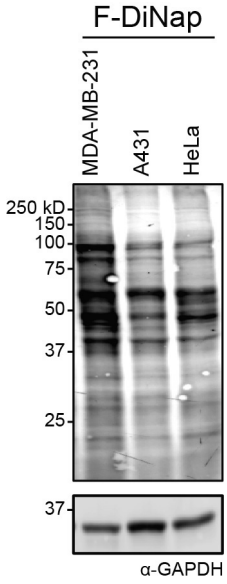

Figure S17. Time-dependent ratiometric labeling of CH-27 B-cells.

Adherent cells were labeled with H-DiNap or F-DiNap (1 mM) and ratiometric images (image collected with 488 nm excitation/image collected with 405 nm excitation) were measured at 2-minute increments at room temperature in Tyrodes buffer. Image size is 81 μm x 81 μm.

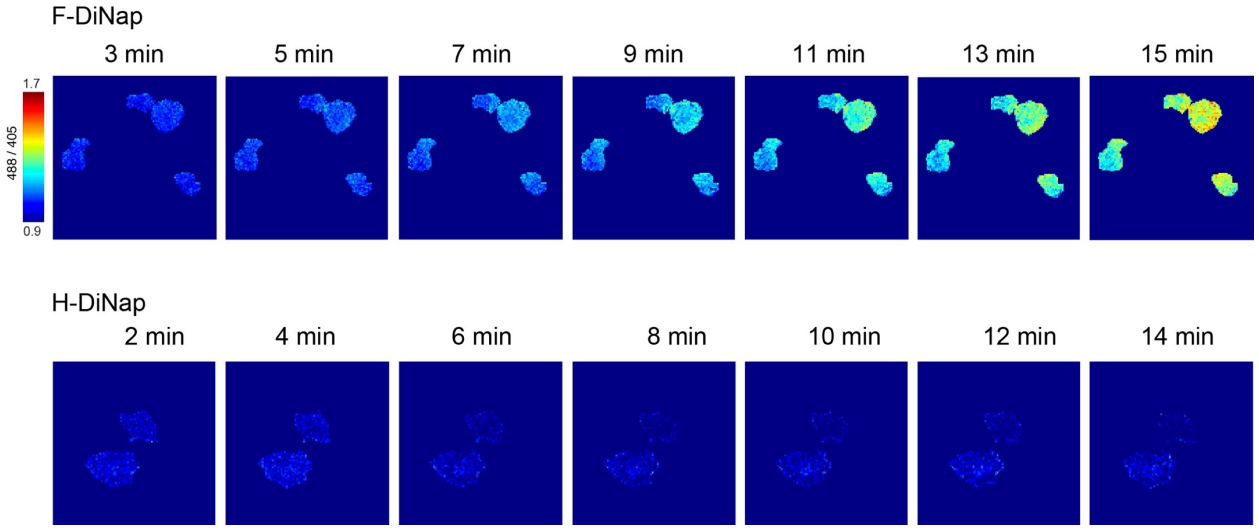

Figure S18. Hydrogen peroxide rapidly increases F-DiNap ratios.

CH27 B-cells were treated with F-DiNap (1 mM) for 15 minutes prior before stimulation and imaged by TIRF microscopy. To stimulate redox stress, hydrogen peroxide (1 mM final) was added. An immediate increase is observed in the 488 nm/405 nm excitation ratio. Scale bar = 20 μm.

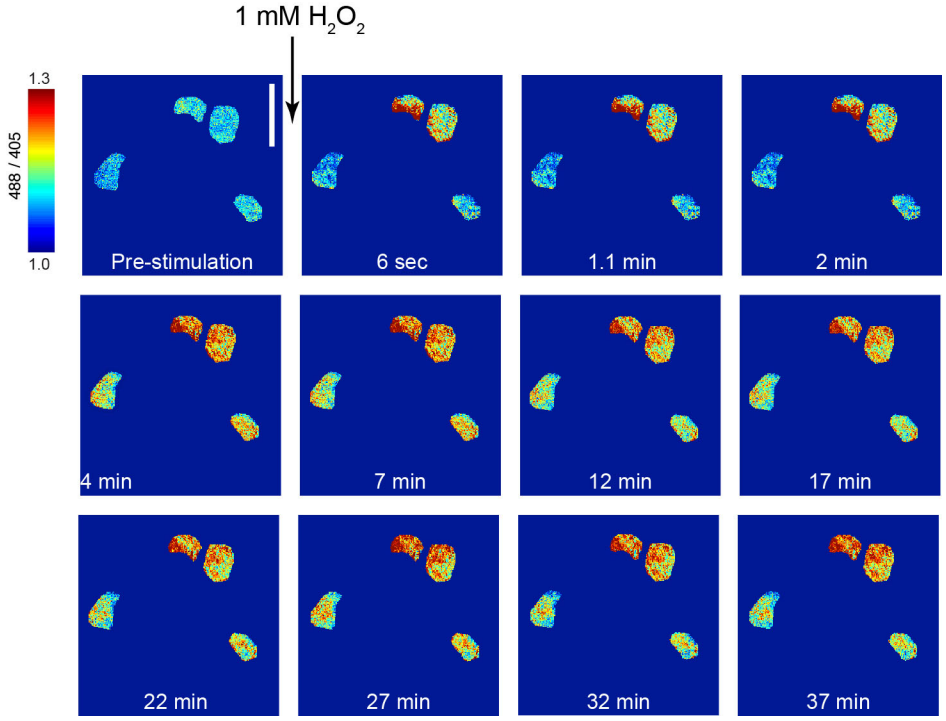

V. NMR spectra

^{1}H NMR: DiNapBr (**2a**)

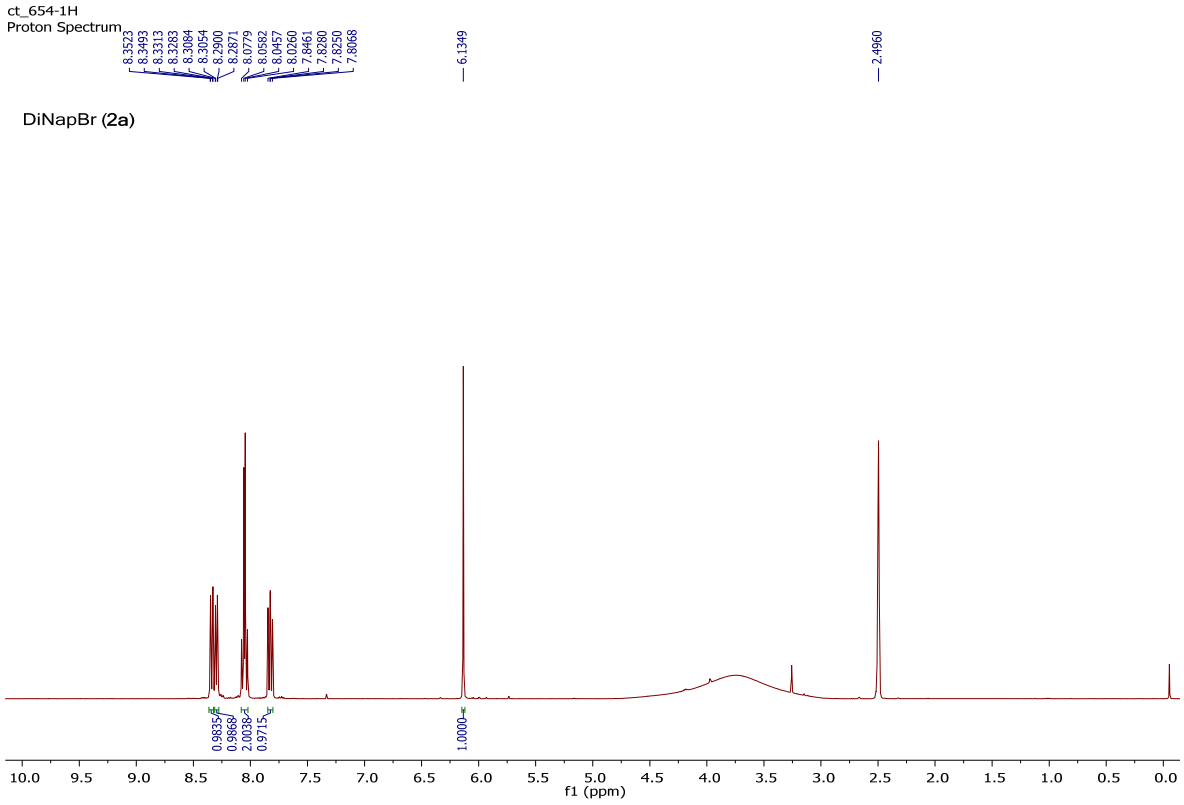

^{13}C NMR: H-DiNapBr (**2a**)

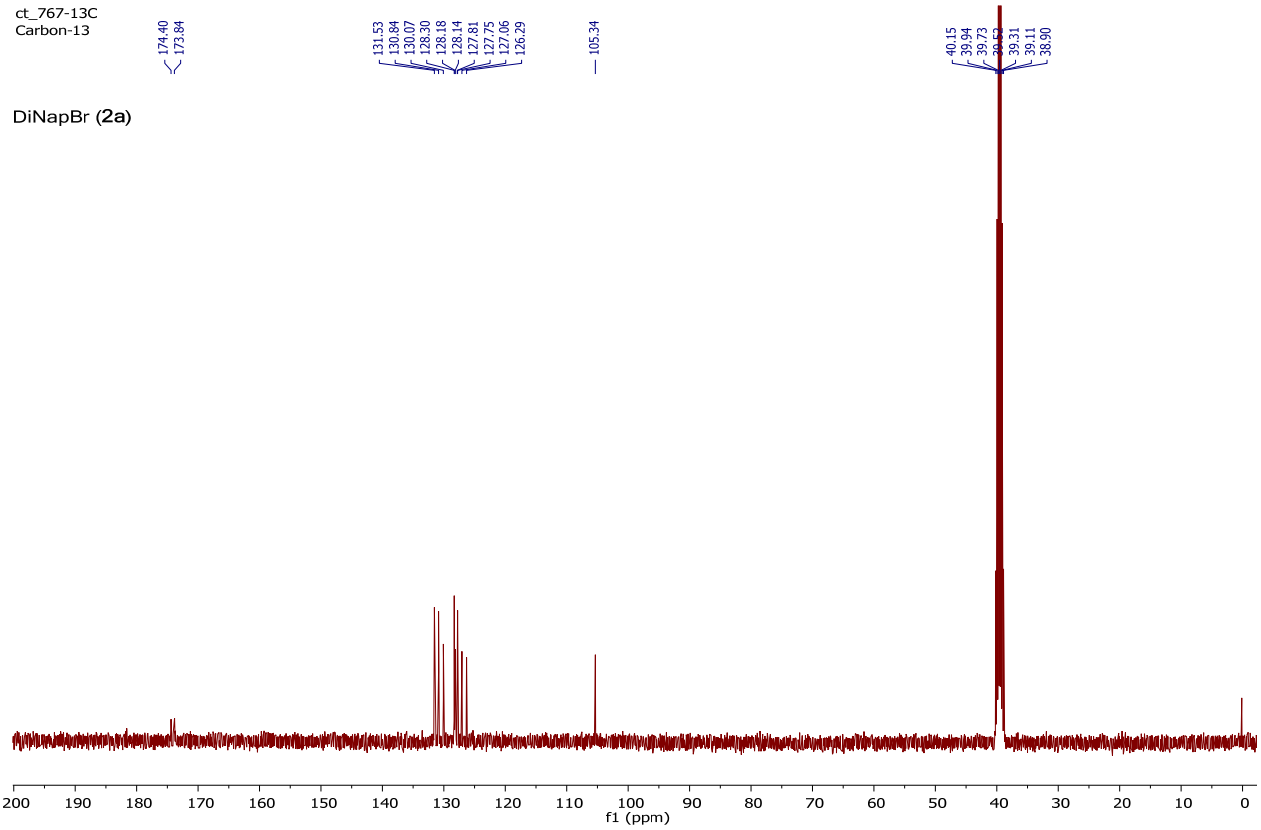

^{1}H NMR: Me-DiNapBr (**2b**)

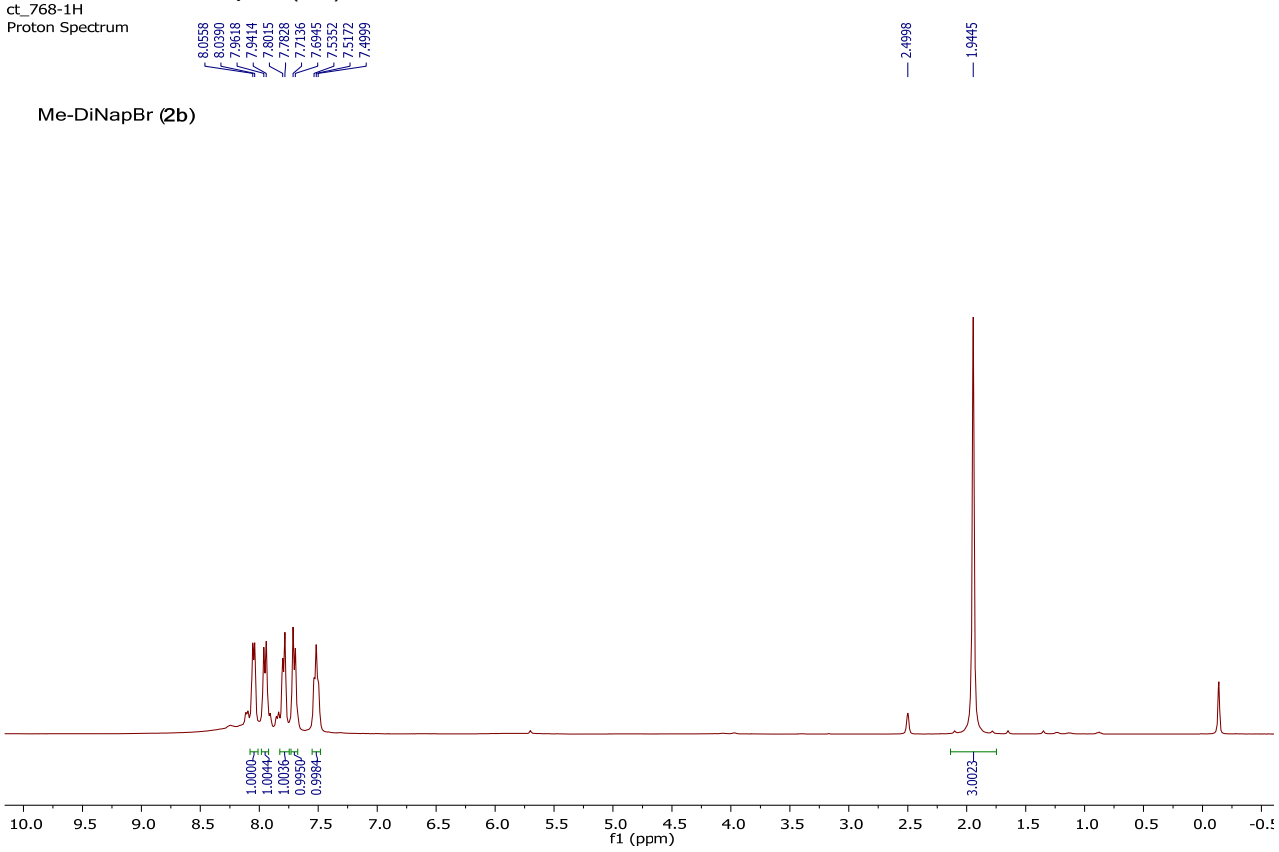

^{13}C NMR: Me-DiNapBr (**2b**)

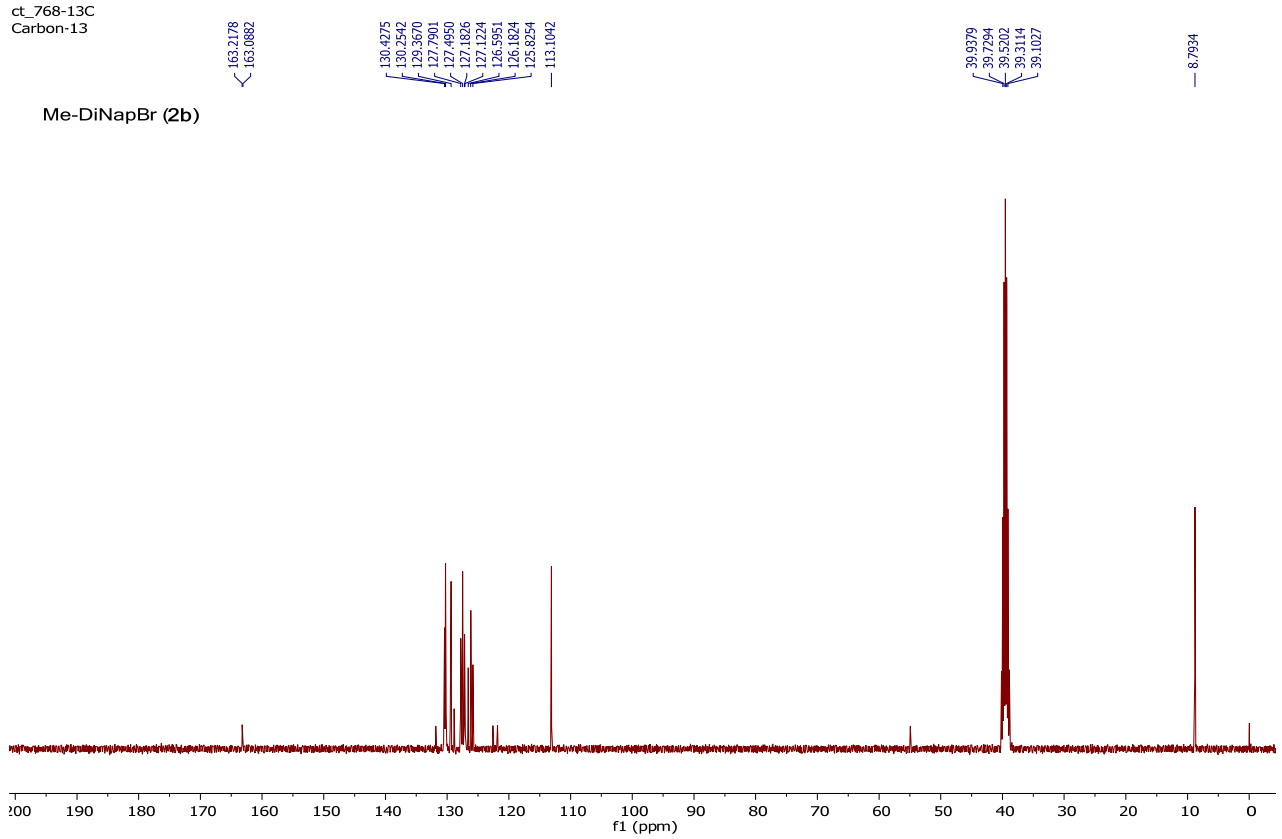

^{1}H NMR: F-DiNapBr (**2c**)

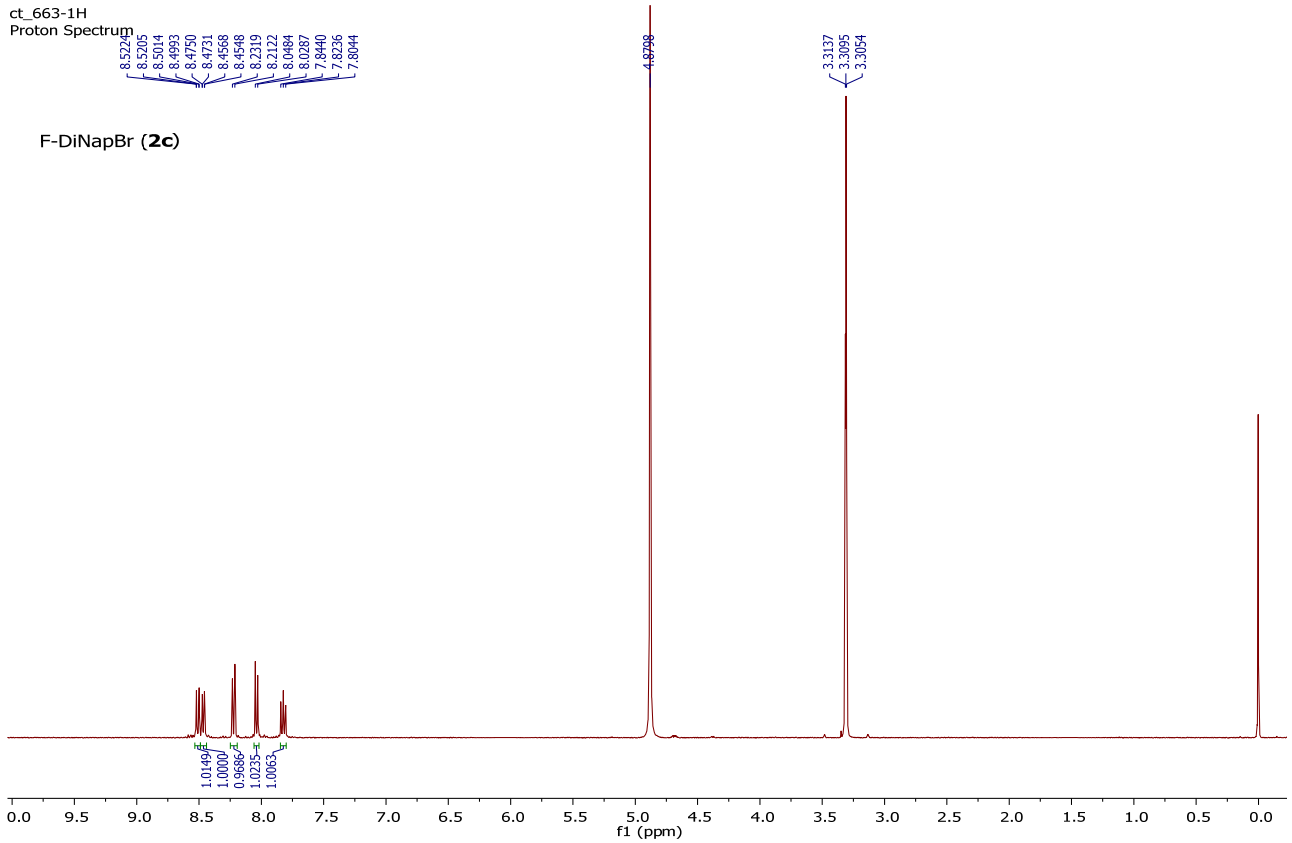

^{13}C NMR: F-DiNapBr (**2c**)

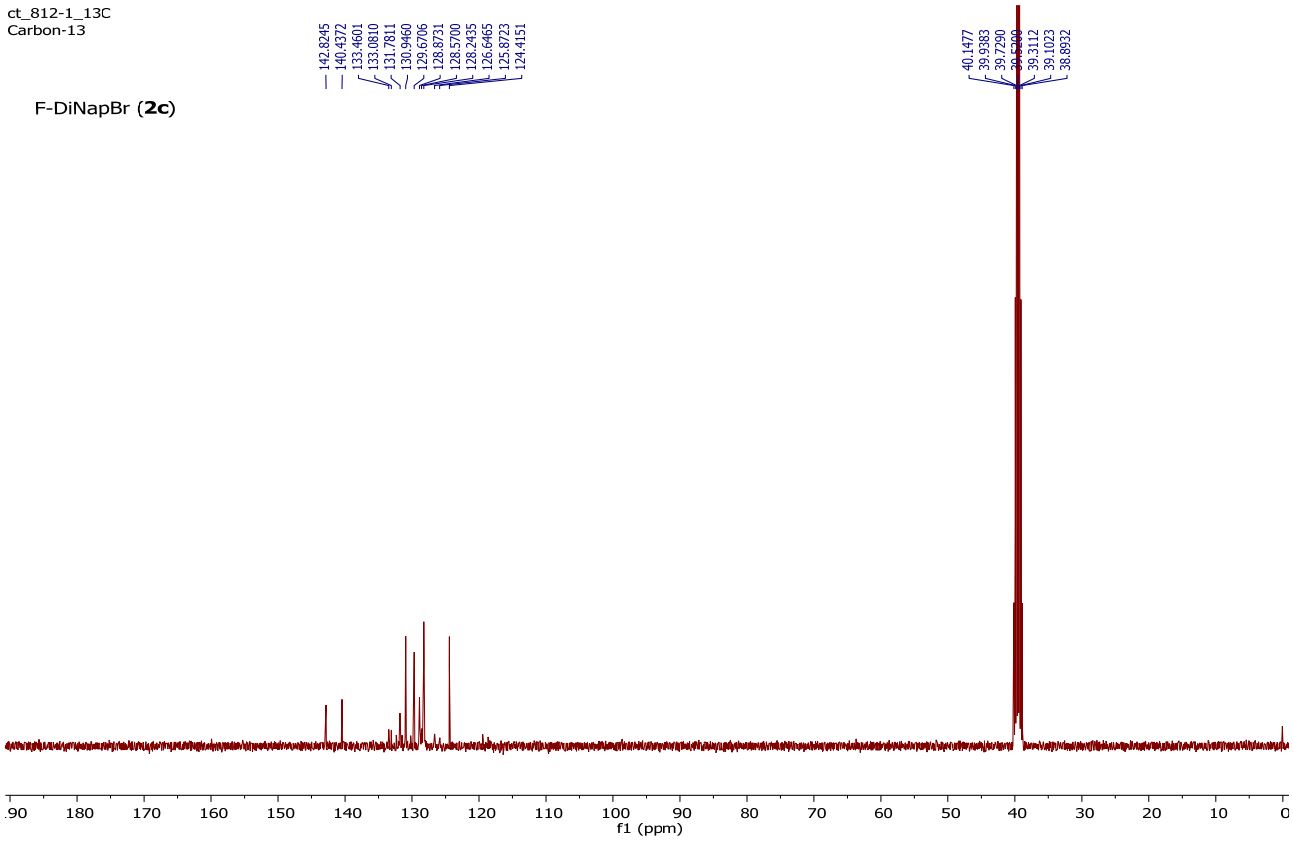

^{19}F NMR: F-DiNapBr (**2c**)

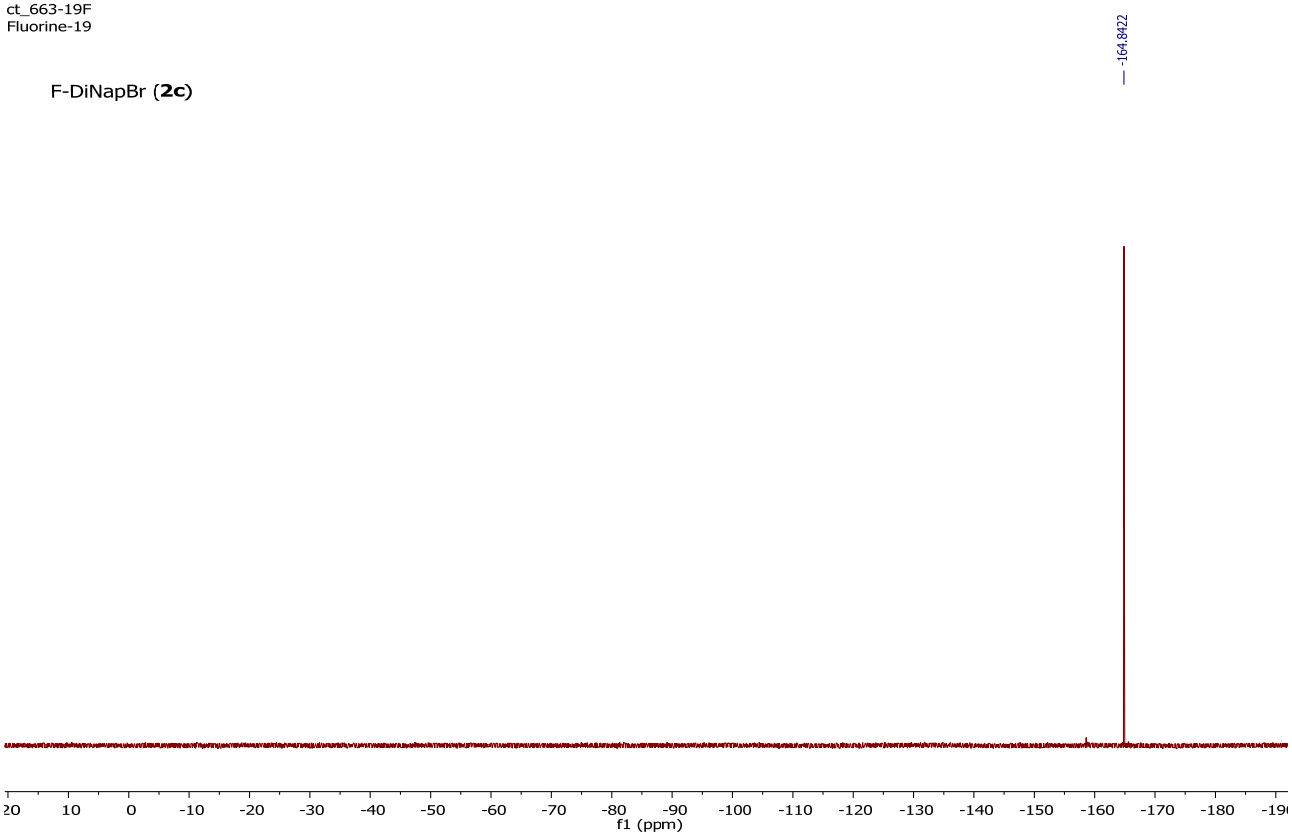

^{1}H NMR: F-DiNapNO$_2$ (**2d**)

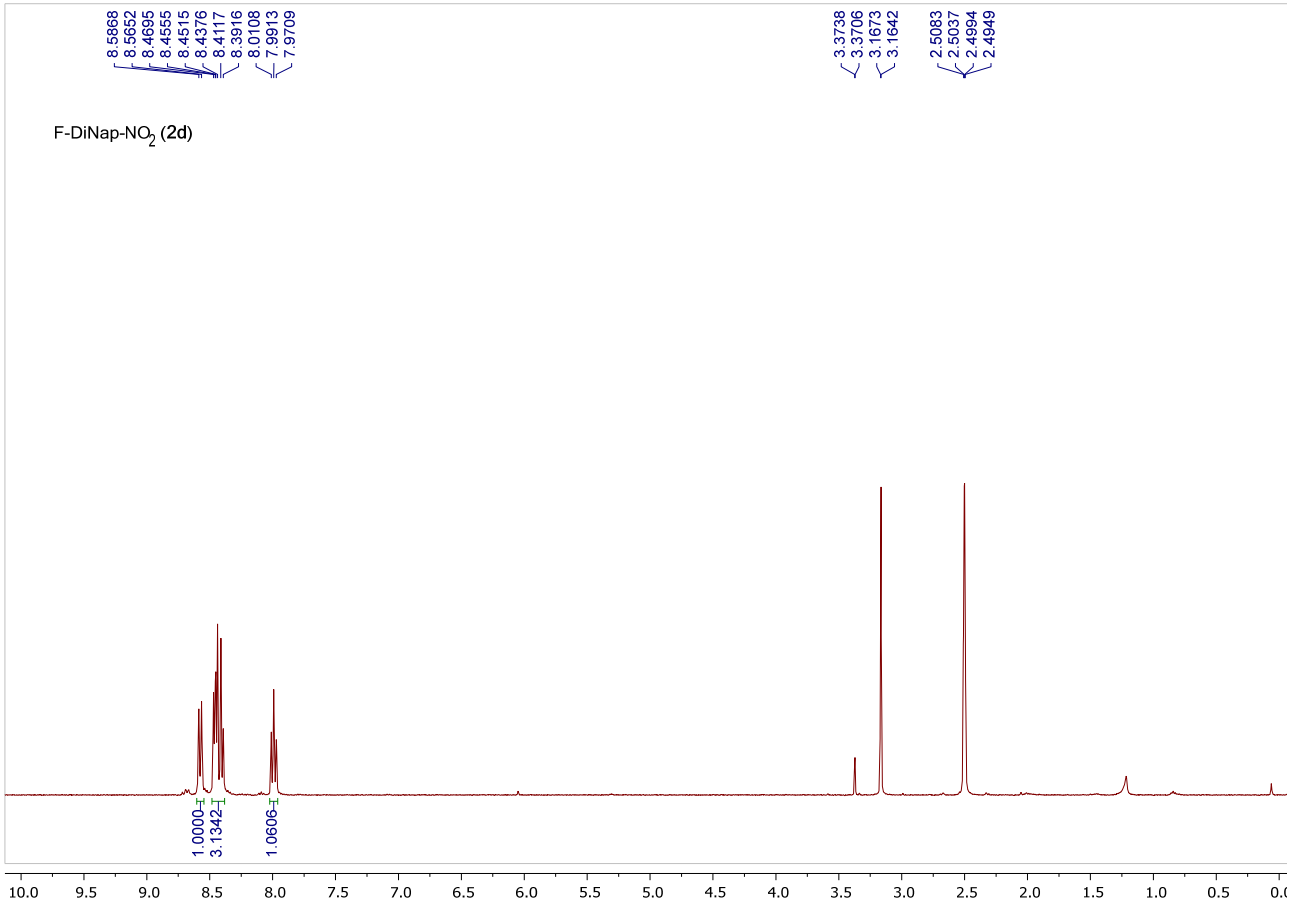

^{13}C NMR: F-DiNapNO$_2$ (**2d**)

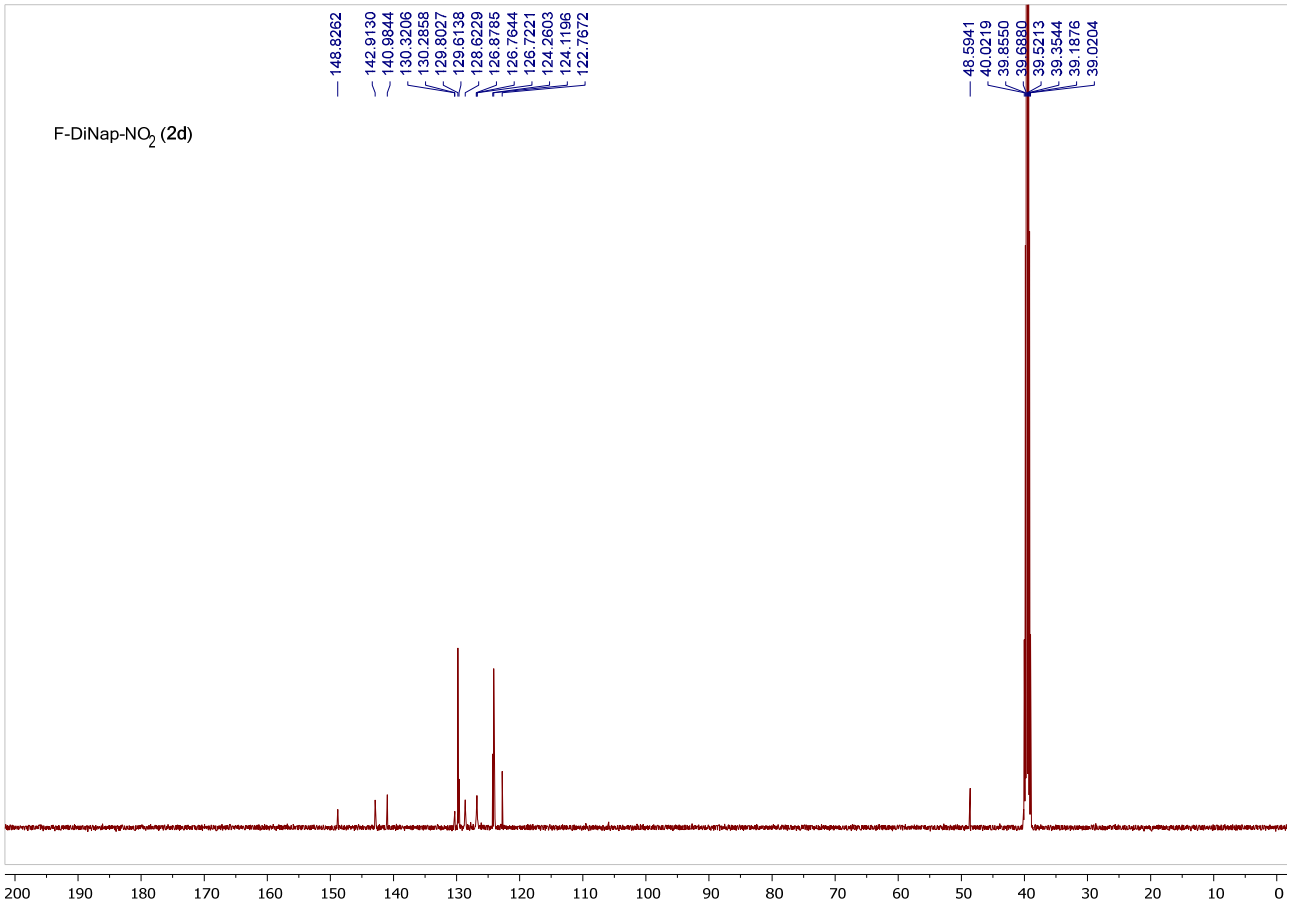

^{19}F NMR: F-DiNapNO_2 (**2d**)

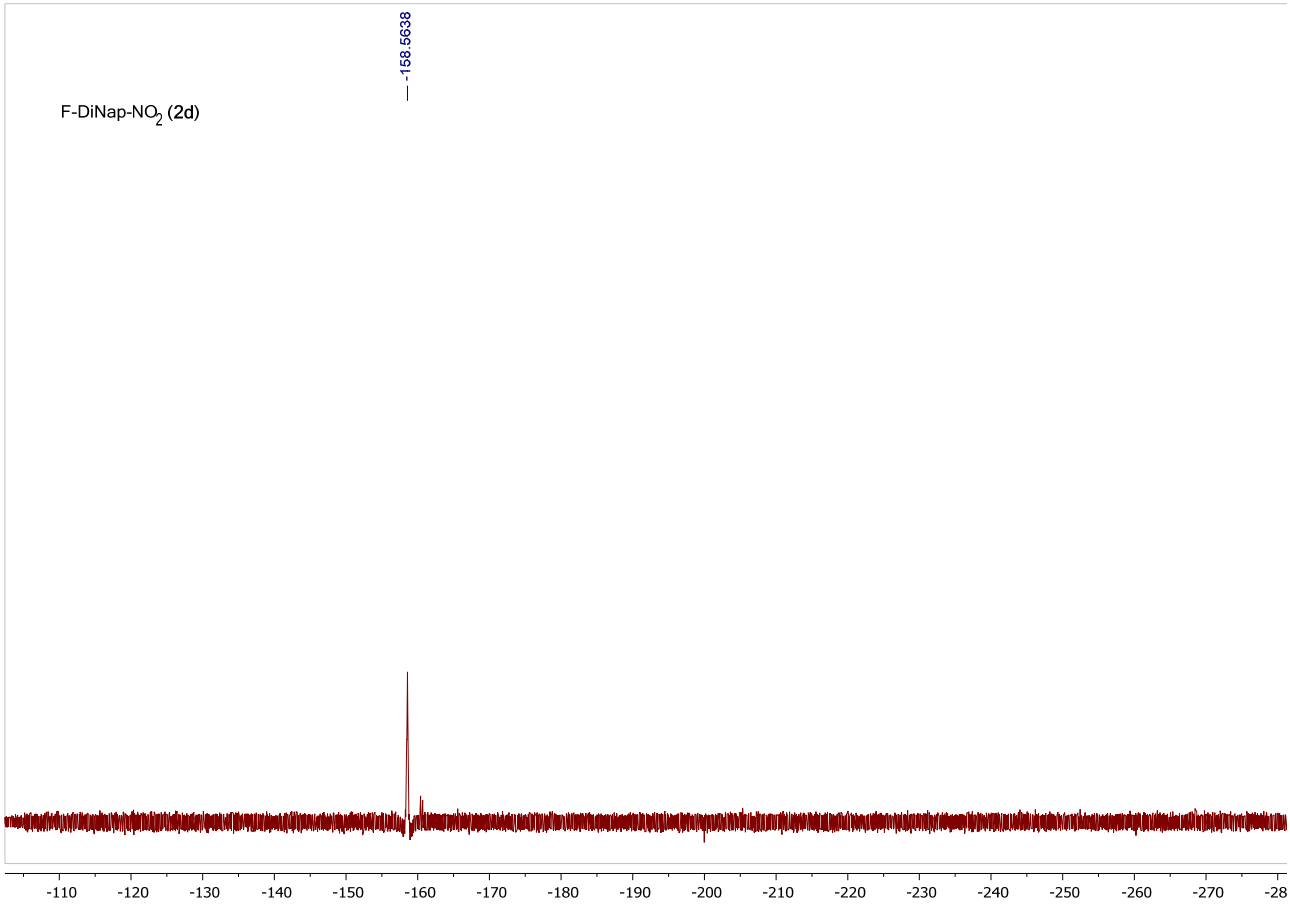

^{1}H NMR: H-DiNapNO$_2$ (**2e**)

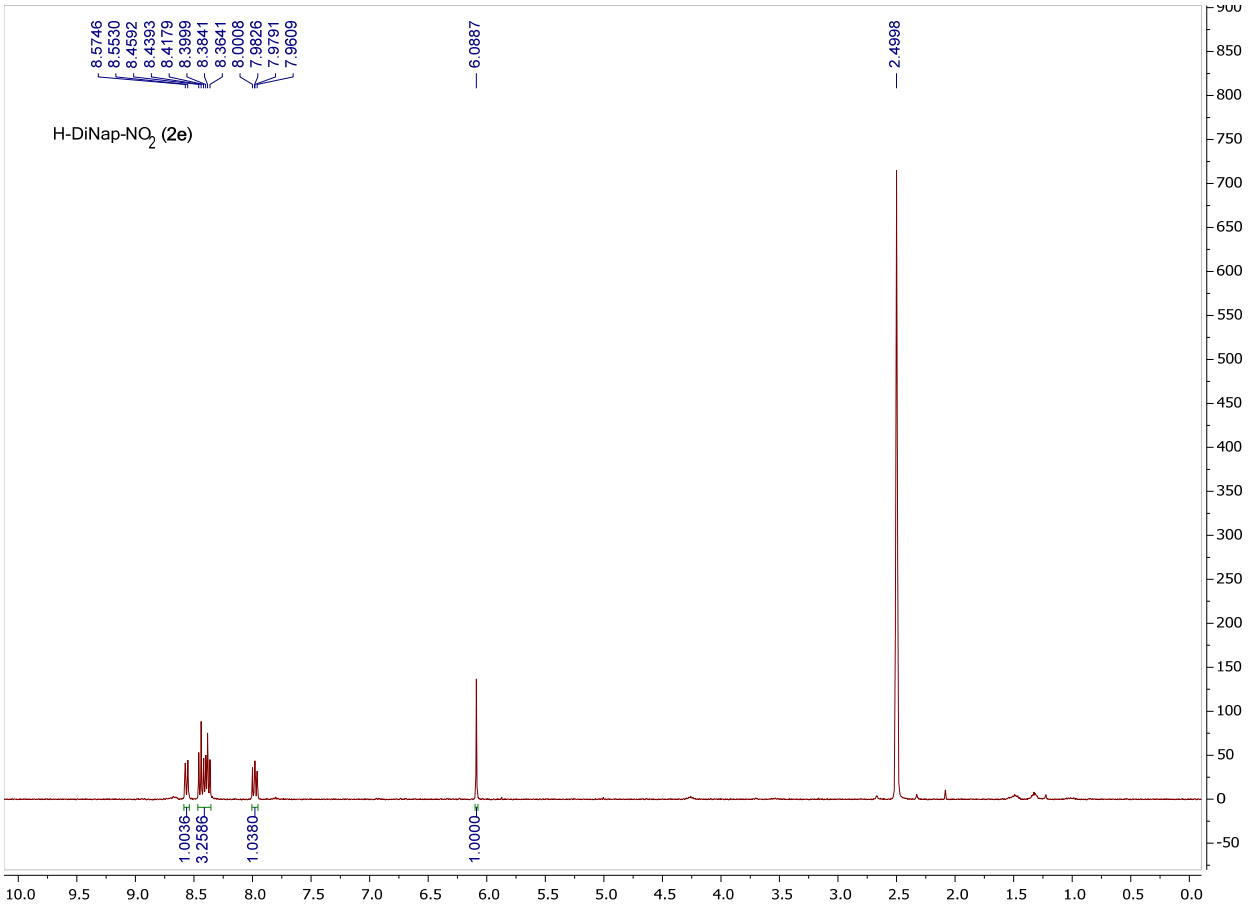

^{13}C NMR: H-DiNapNO$_2$ (**2e**)

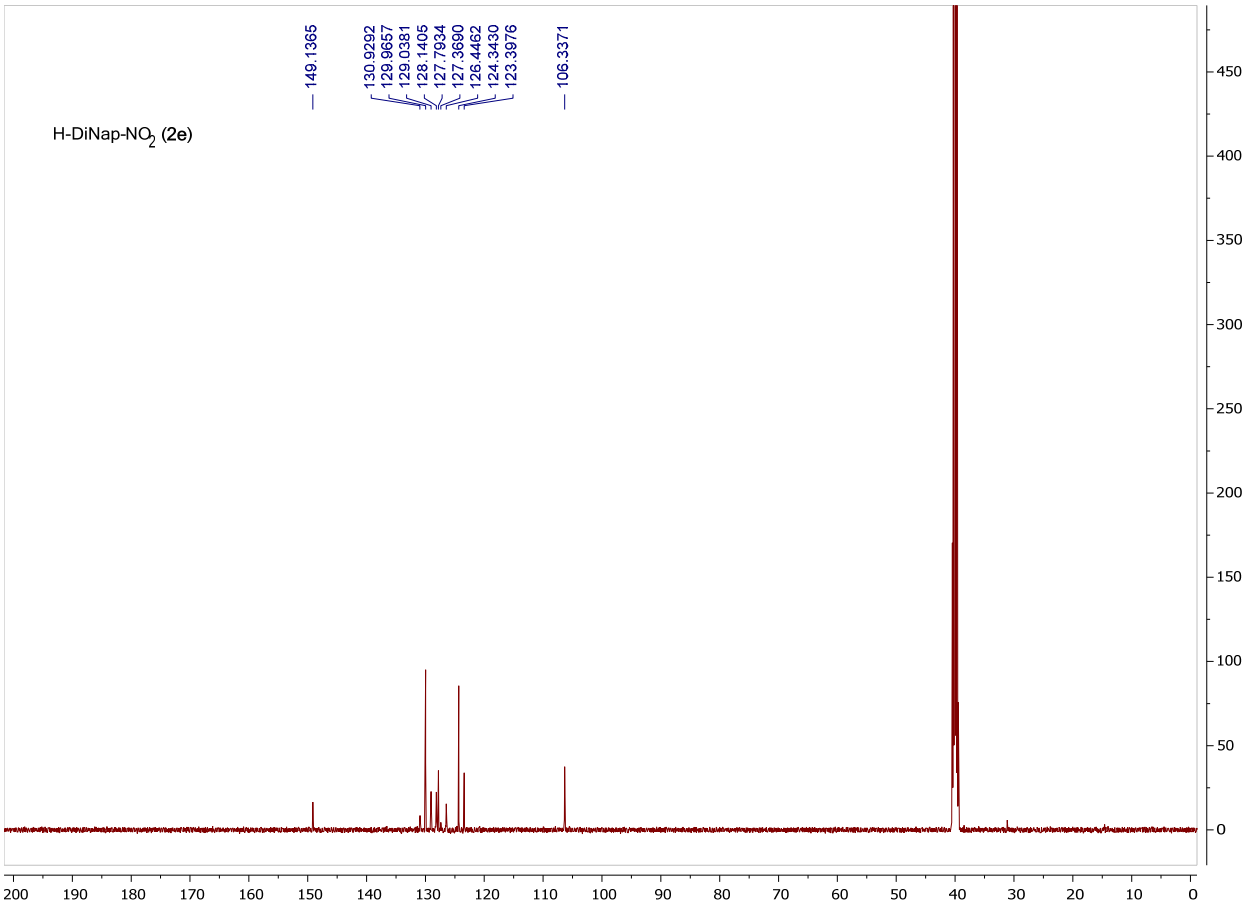

^{1}H NMR: H-DiNap (**3a**)

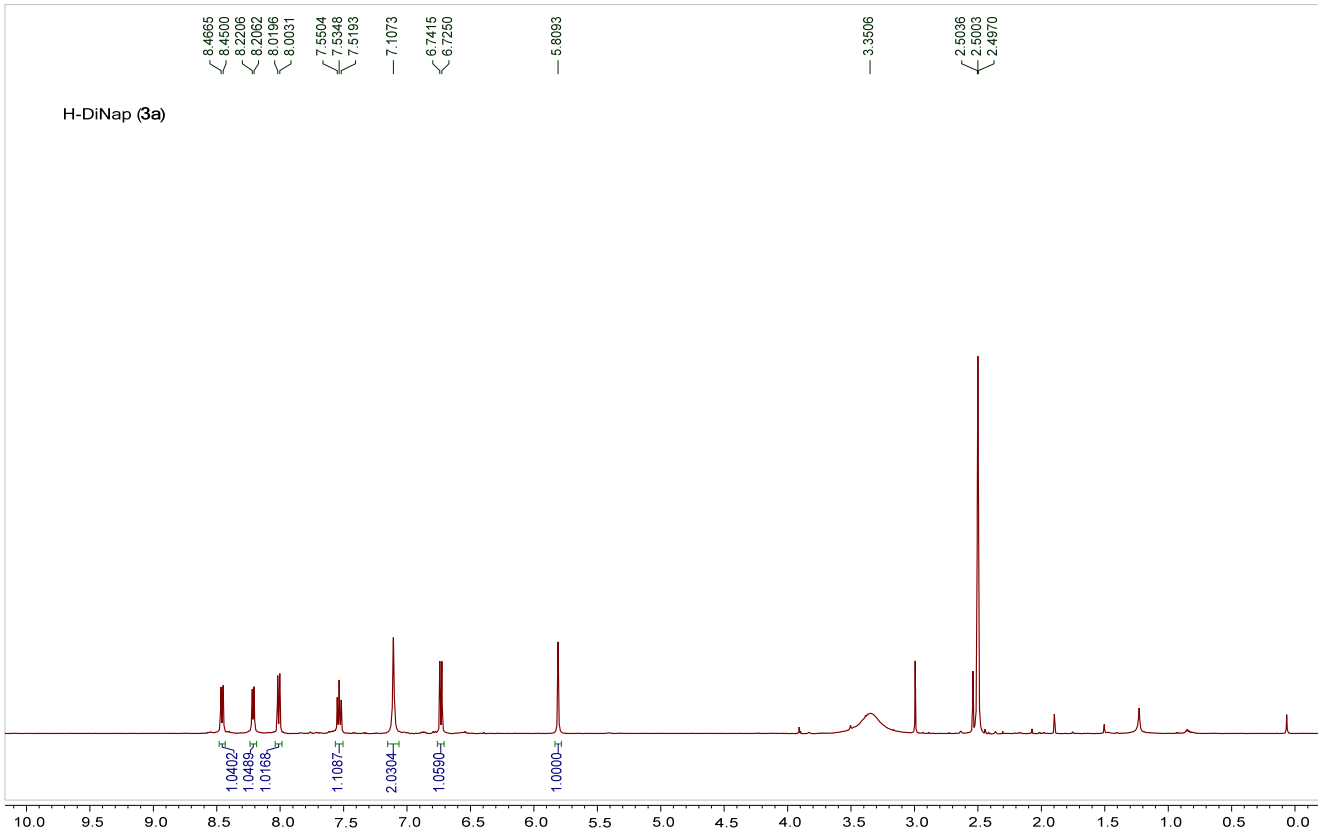

^{13}C NMR: H-DiNap (**3a**)

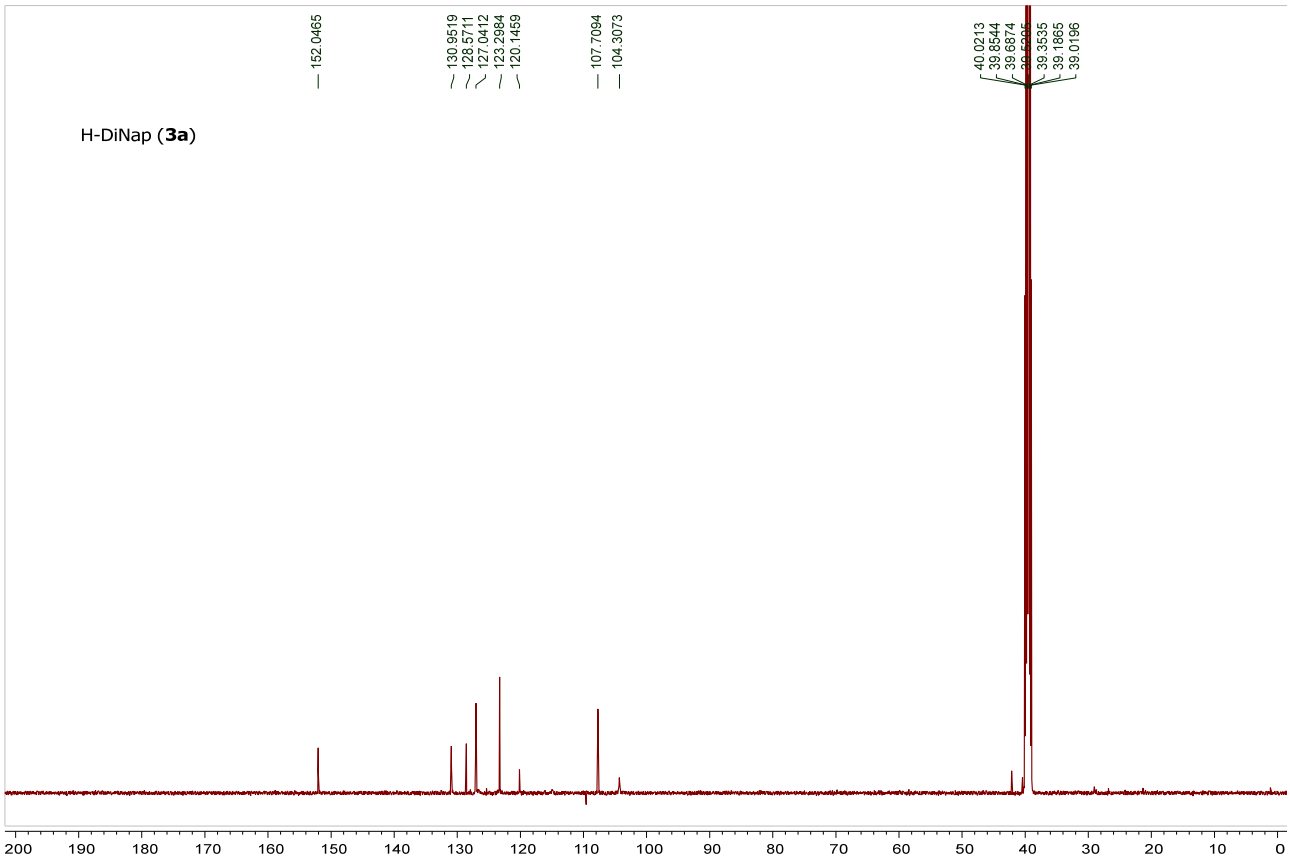

^{1}H NMR: Me-DiNap (**3b**)

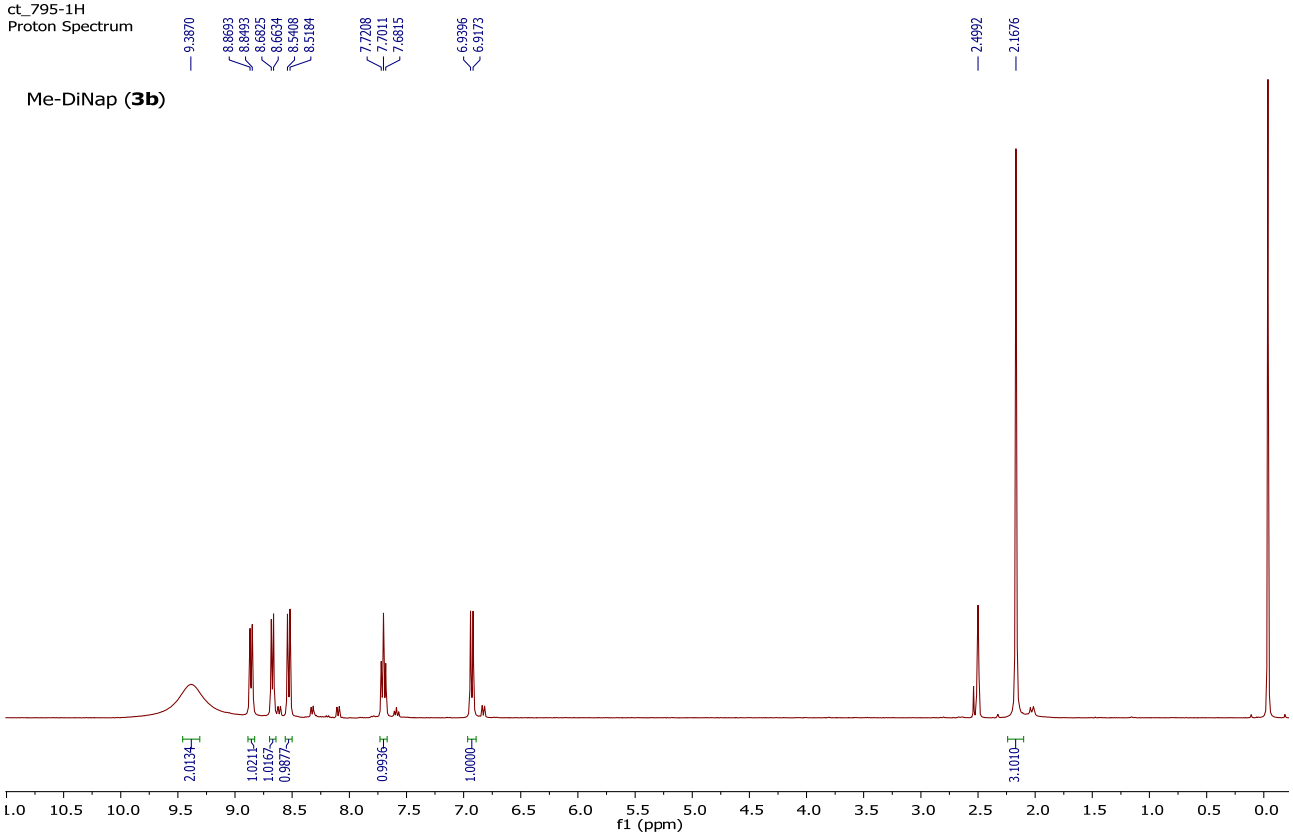

^{13}C NMR: Me-DiNap (**3b**)

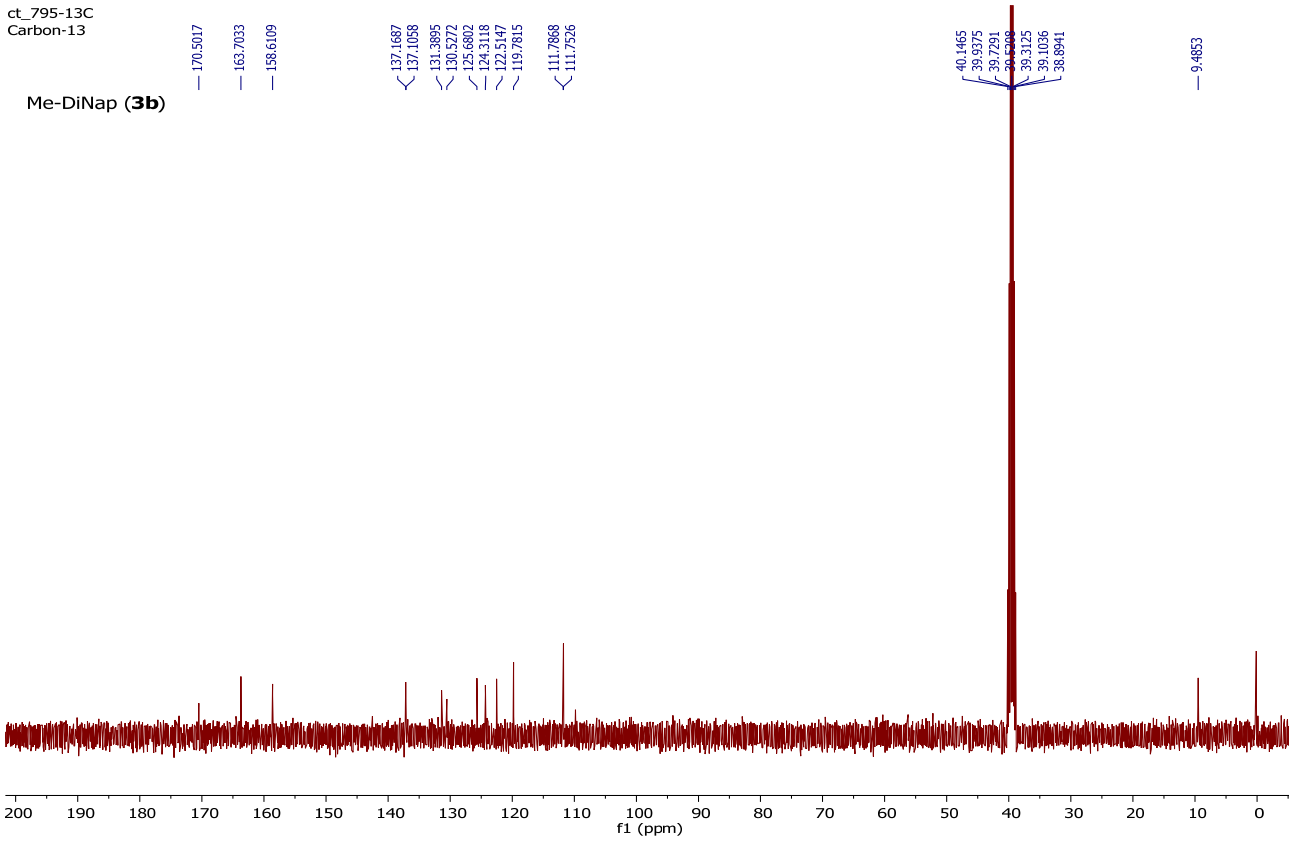

^{1}H NMR: F-DiNap (**3c**)

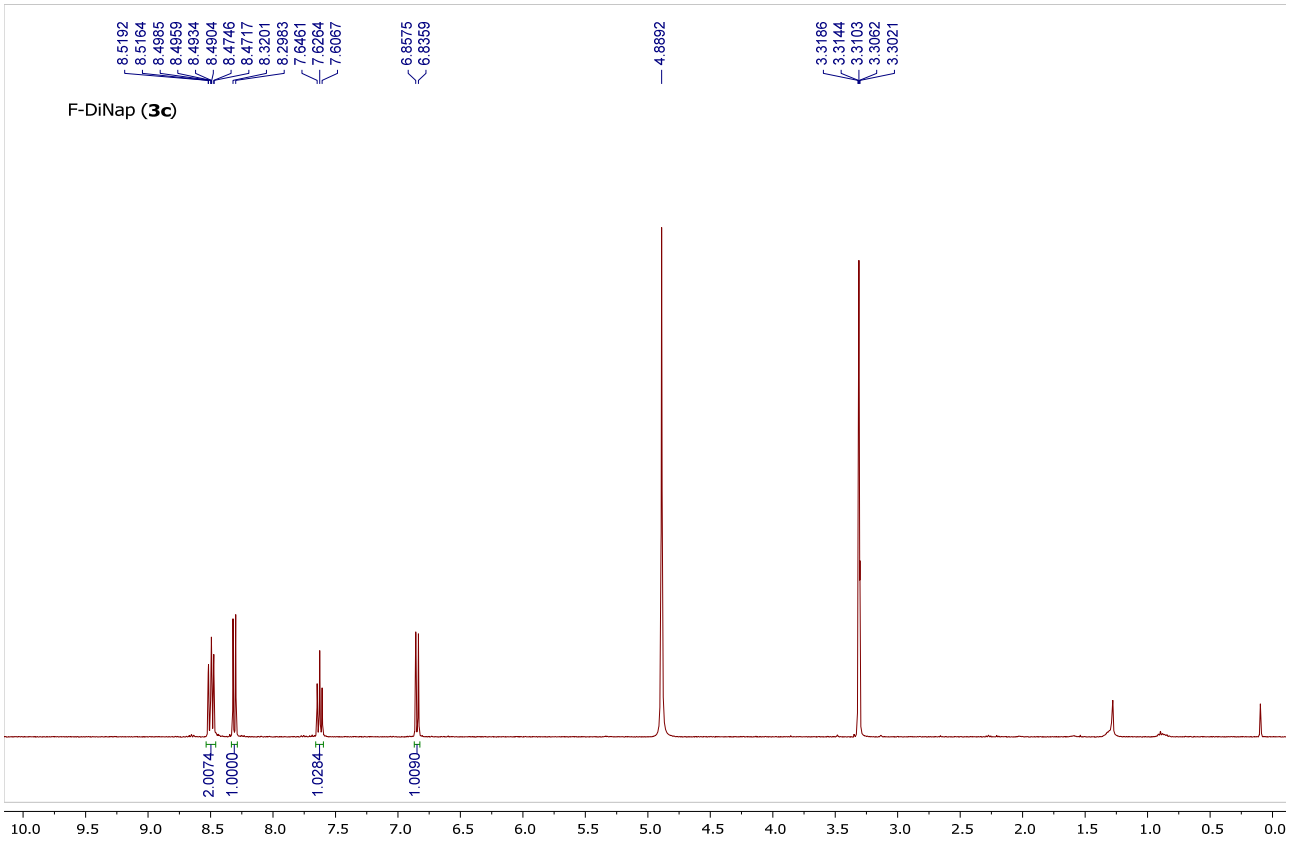

^{13}C NMR: F-DiNap (**3c**)

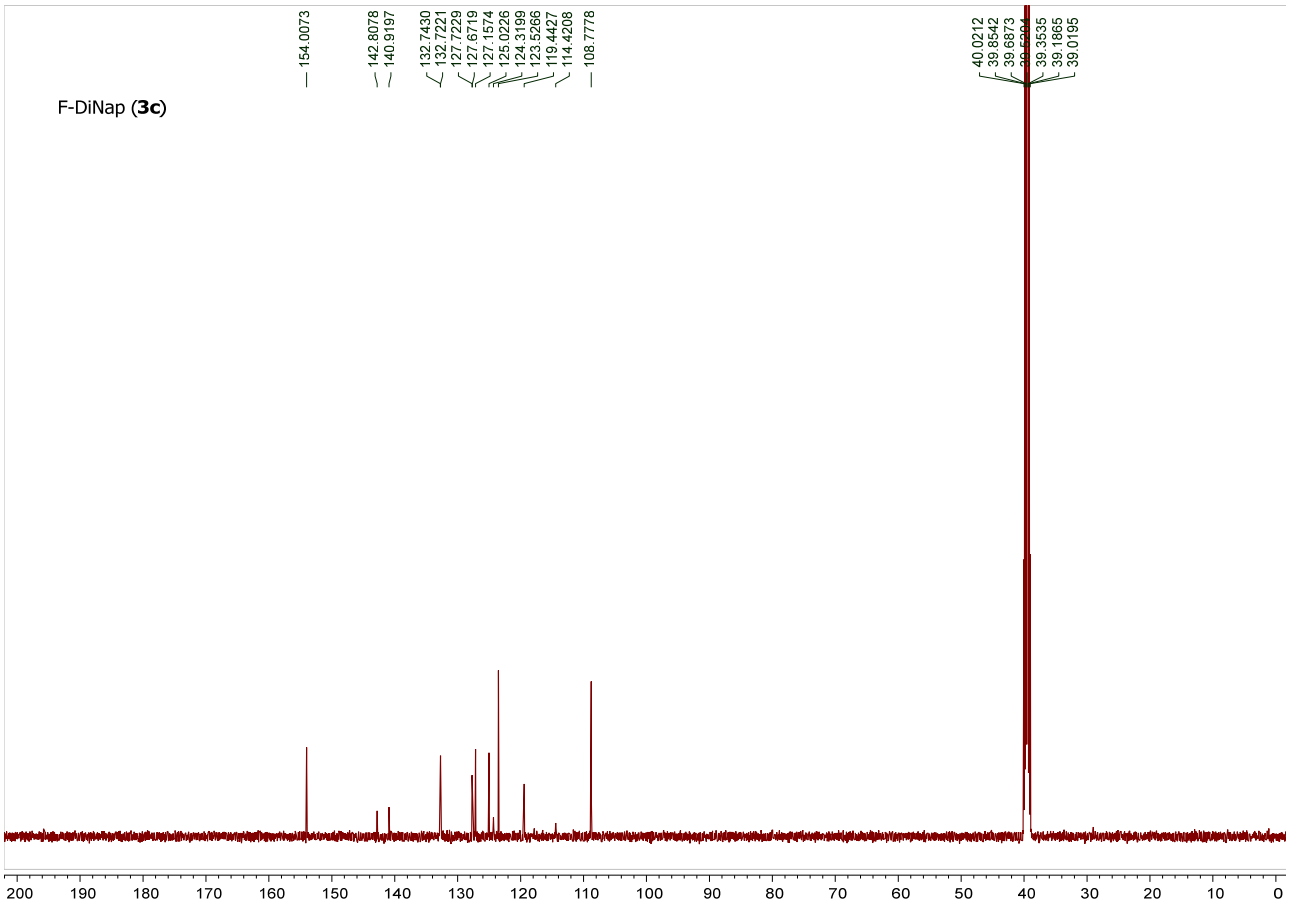

^{19}F NMR: F-DiNap (**3c**)

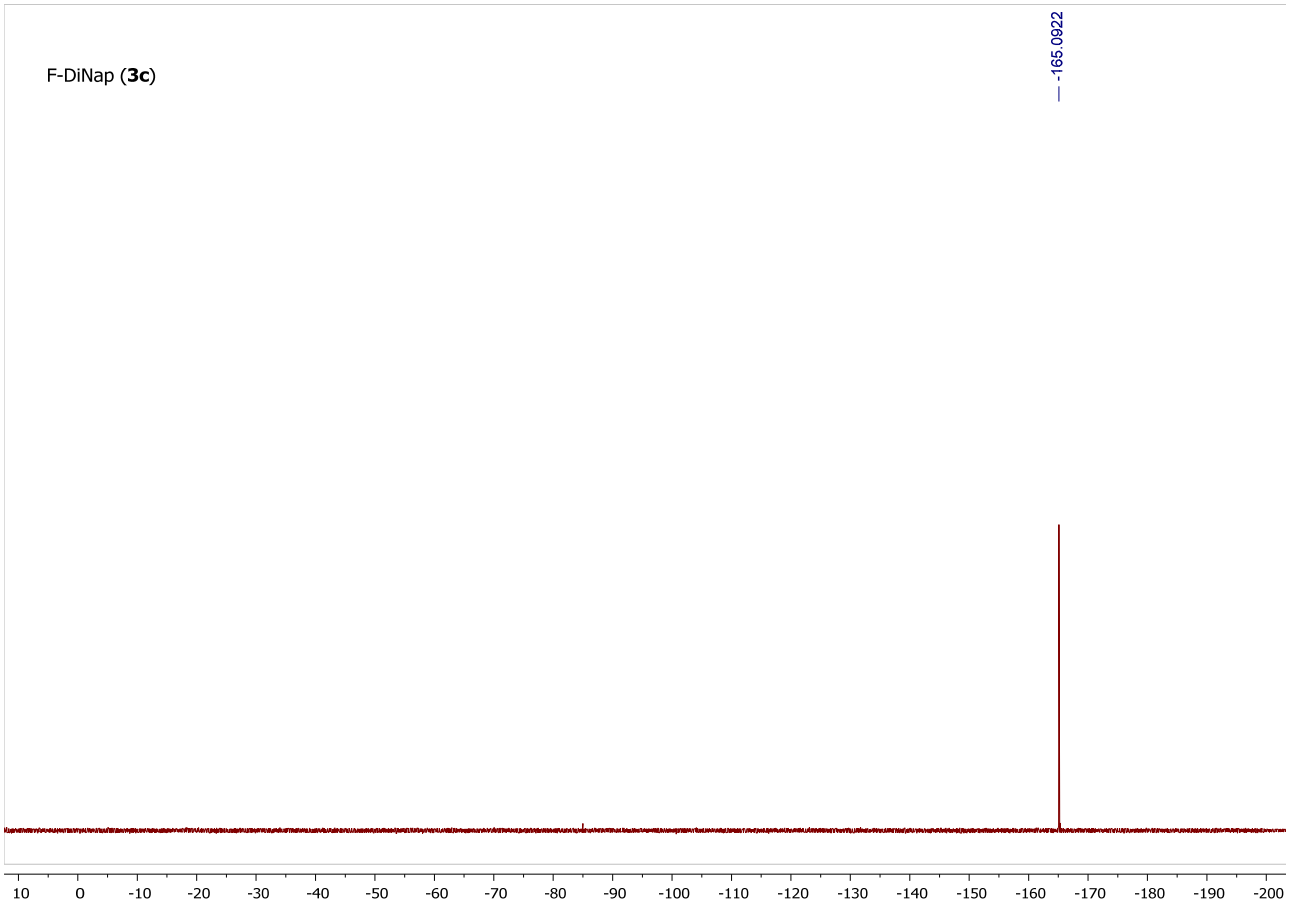

^{1}H NMR: *S*-Me-H-DiNap (**4a**)

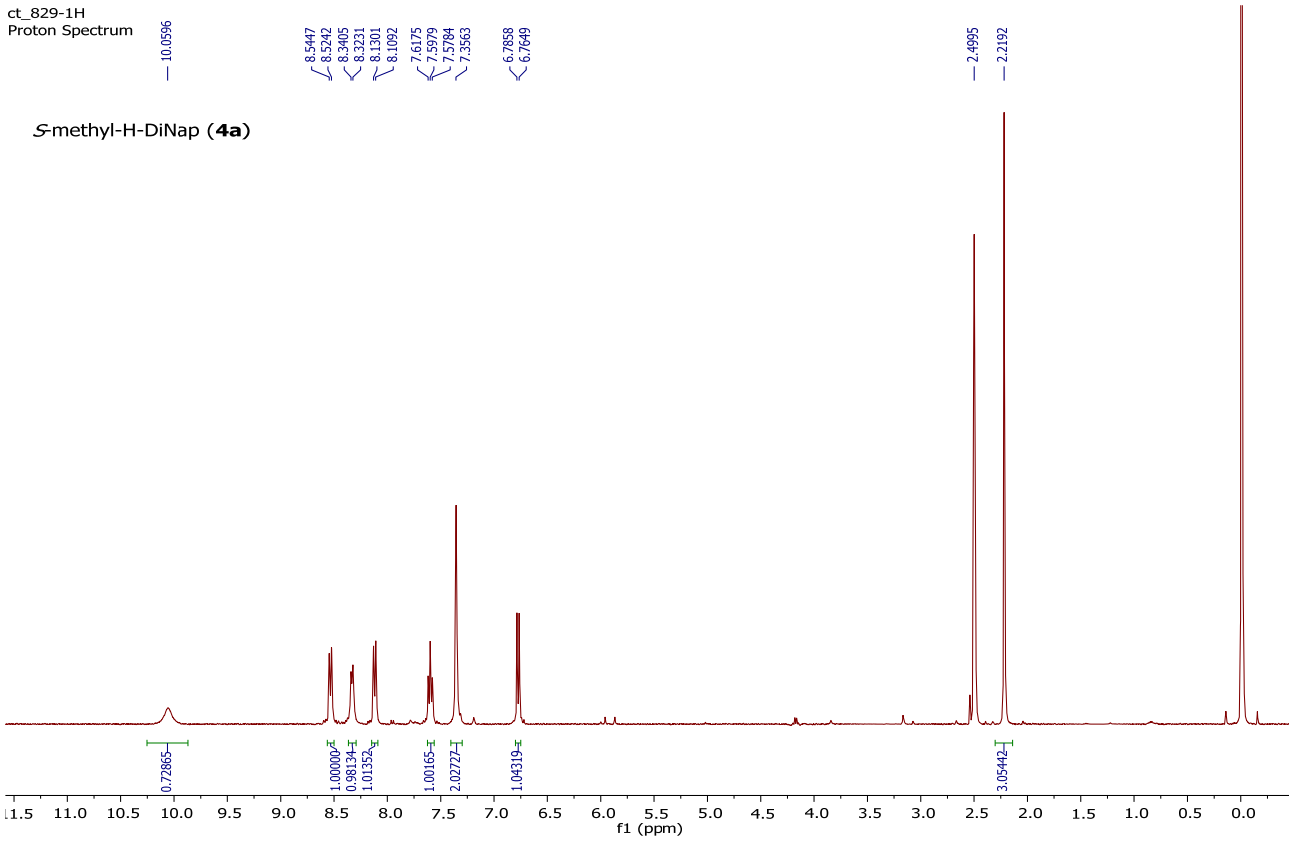

^{13}C NMR: *S*-Me-H-DiNap (**4a**)

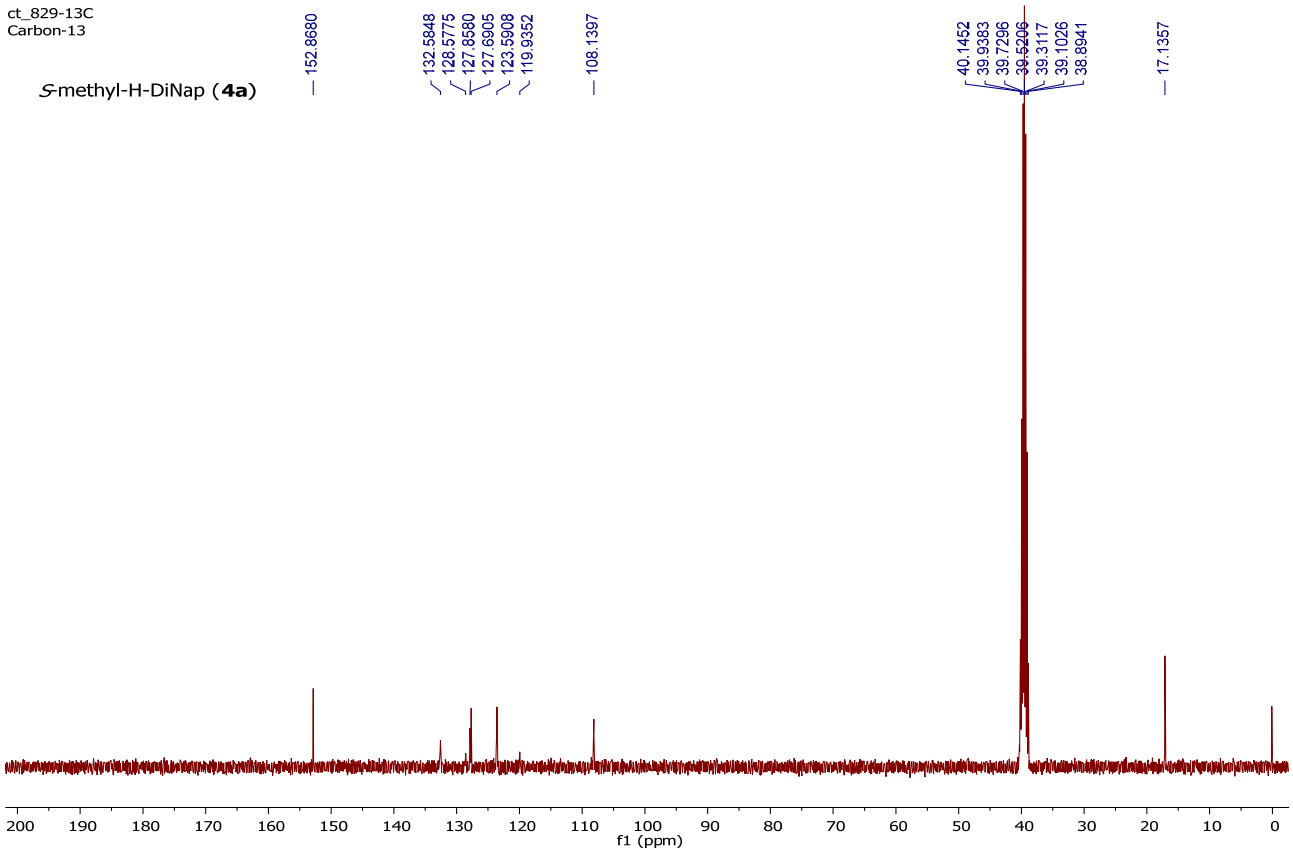

^{1}H NMR: *S*-Me-F-DiNap (**4c**)

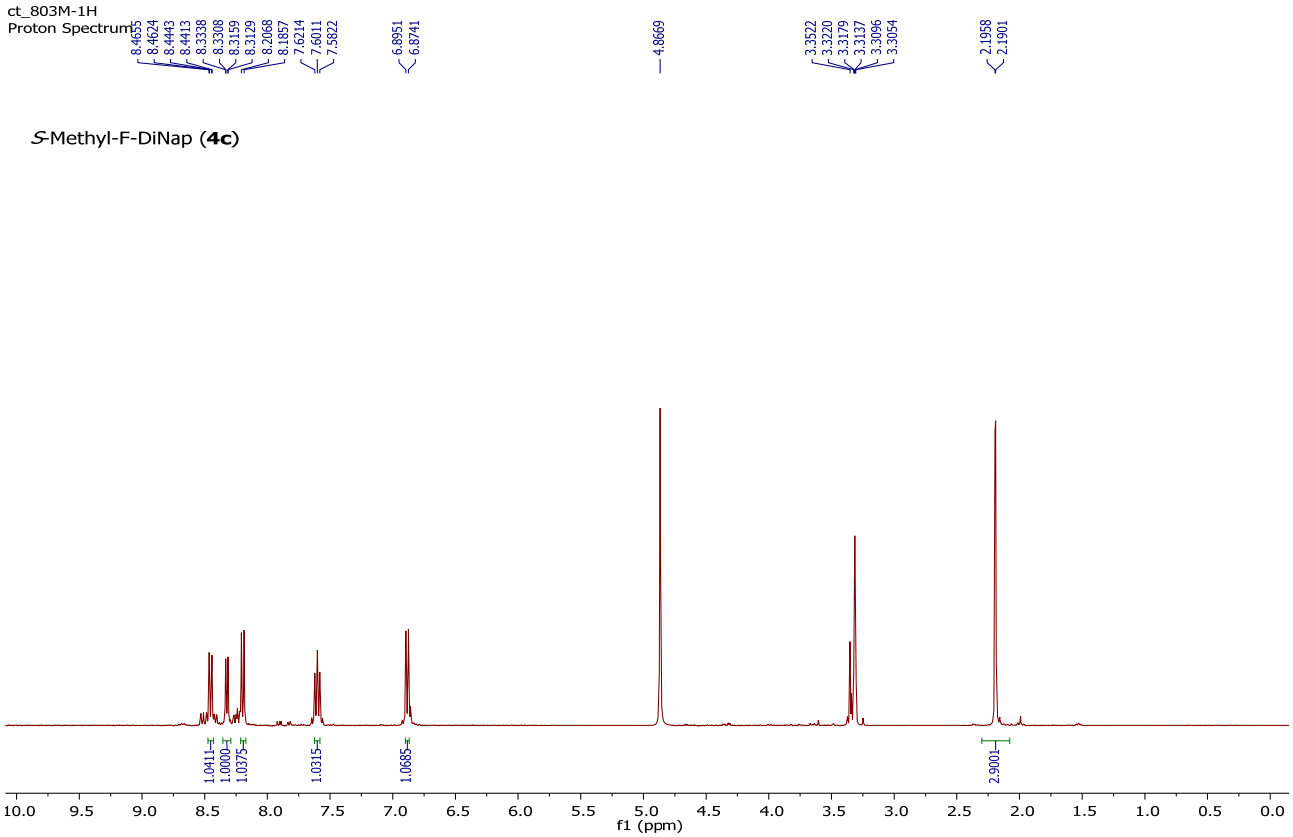

S-Methyl-F-DiNap (**4c**)

^{19}F NMR: *S*-Me-F-DiNap (**4c**)

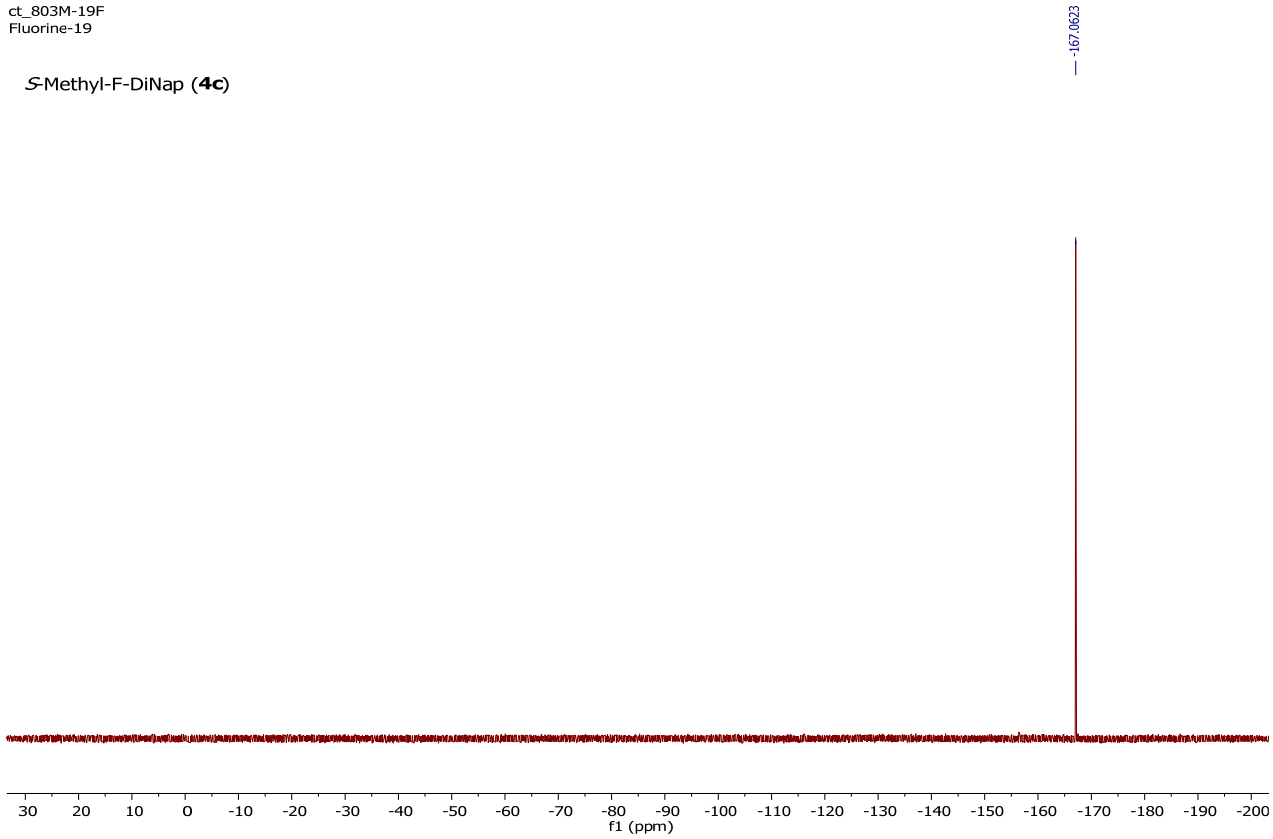

^{19}F NMR: FDiNap (**3c**) in PBS/10% D_2O

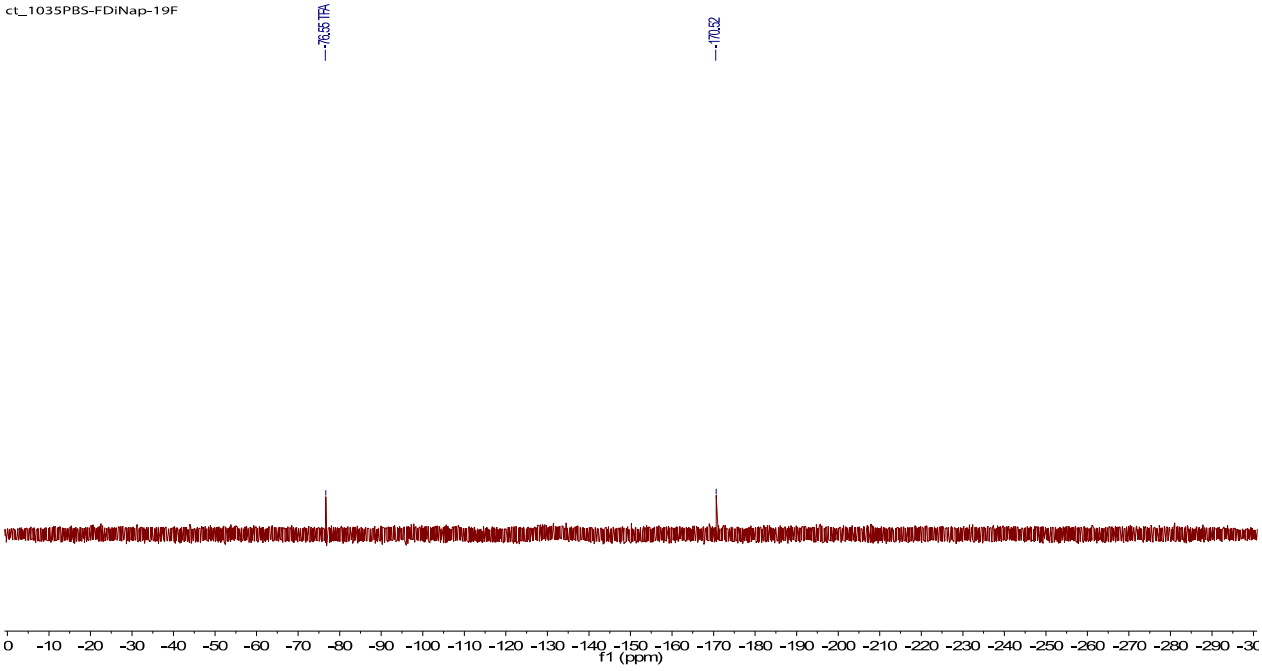

^{19}F NMR: F-DiNap and MeOVal-CysSA-Cbz in PBS/10% D_2O

ct_1035PBS-FDiNap + SA-19F

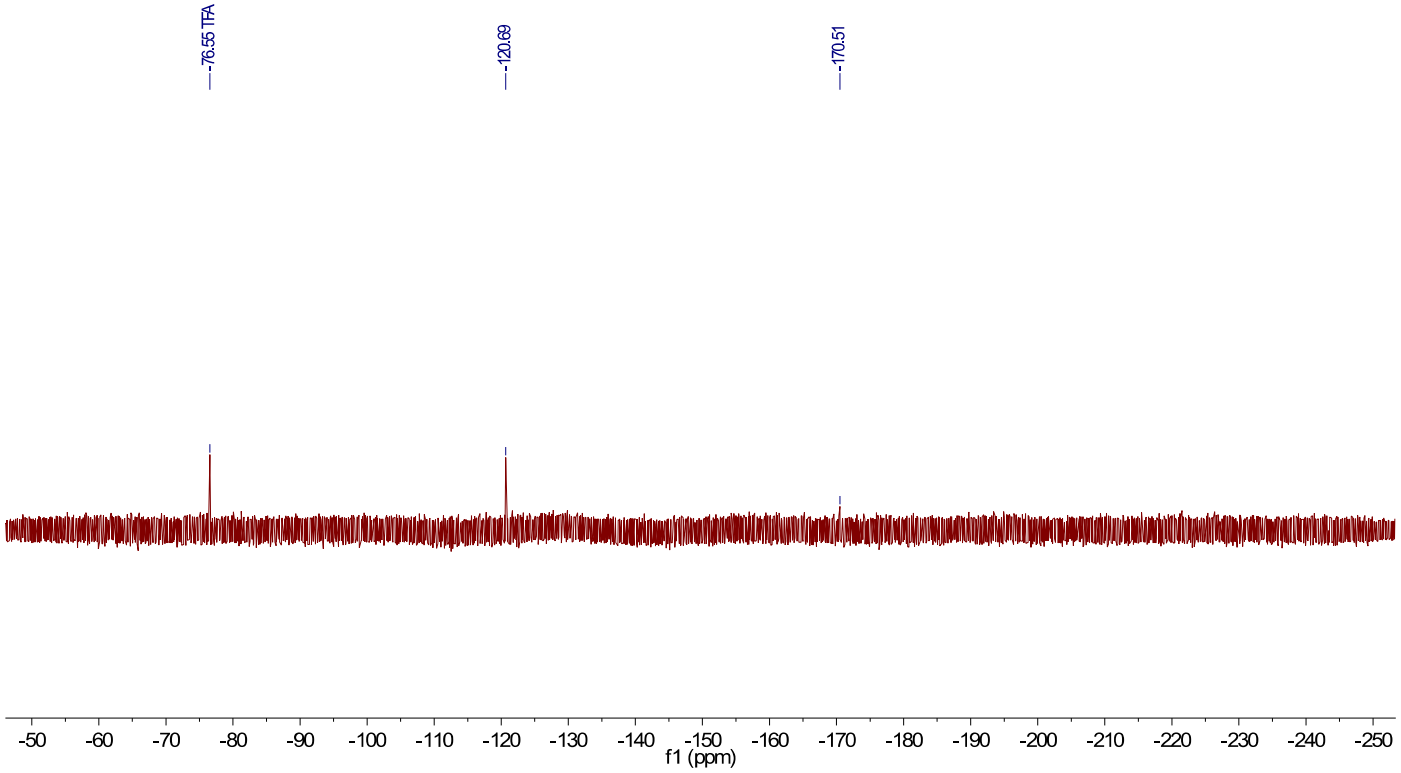

VI. HPLC Spectra

HPLC trace of H-DiNap (**3a**). Absorbance at 488 nm.

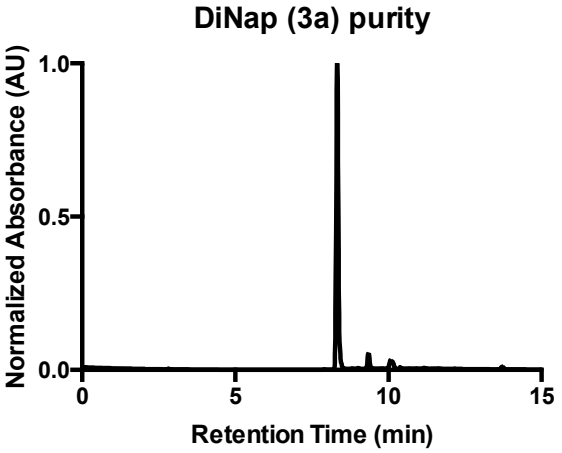

HPLC trace of Me-DiNap (**3b**). Absorbance at 488 nm.

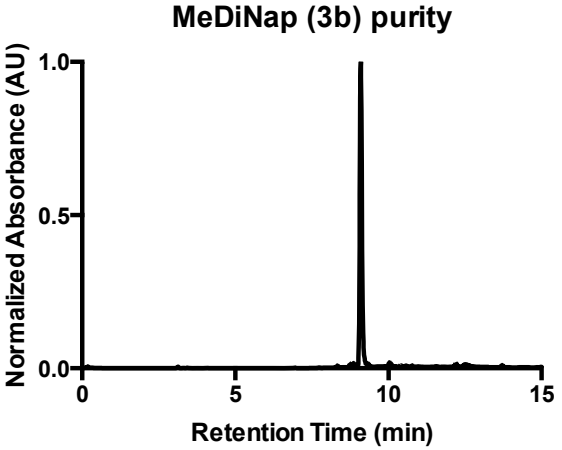

HPLC trace of F-DiNap (**3c**). Absorbance at 488 nm.

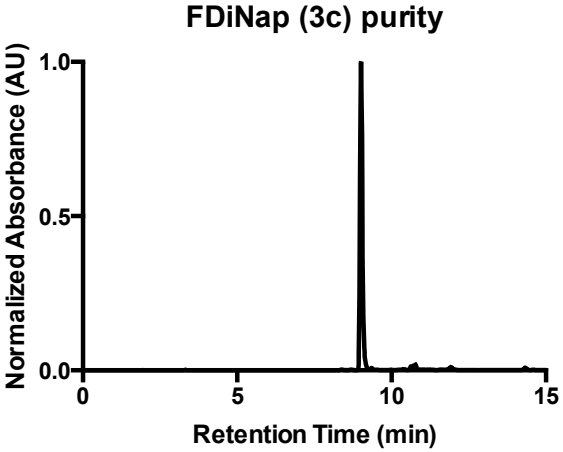

VII. References

[1] H. E. Gottlieb, V. Kotlyar, A. Nudelman, *J. Org. Chem.* **1997**, *62*, 7512-7515.

[2] L. D. Lavis, T. Y. Chao, R. T. Raines, *Chem. Sci.* **2011**, *2*, 521-530.

[3] M. Fischer, W. Stadlbauer, *J. Het. Chem.* **1997**, *34*, 993-997.

[4] J. T. Markiewicz, O. Wiest, P. Helquist, *J. Org. Chem.* **2010**, *75*, 4887-4890.

[5] V. Gupta, K. S. Carroll, *Chem. Sci.* **2016**, *7*, 400-415.